Roskilde University

Reflection Project

Mathematical Modeling of Blood Cancer

Author:
Katrine Ottesen Bangsgaard,
64421

Supervisor:
Morten Andersen

31 May 2018

Roskilde University
Department of Science and Environment
Universitetsvej 1, Postboks 260
4000 Roskilde, Denmark
Phone +45 4674 2000
ruc@ruc.dk

Abstract

The subject for this project is the disease myeloproliferative neoplasms which is a subtype of blood cancer. The models formulated in this project are based on the model describing the interaction of MPN and the inflammatory system proposed in [1]. The model proposed in [1] is presented and their choice for including a specific T-cell response is reflected upon. In particular their assumption that the death rate of naive T-cells is significantly larger than the amount of malignant stem cells is investigated and a new model is formulated as a modified version of their model with a more complicated T-cell response. The modified model is analysed using the theory of dynamical systems where global existence is guaranteed by establishing a trapping region. A semi analytic investigation reveals that the dynamics of the modified model differs from the model proposed in [1] if the mentioned assumption does not hold. This finding is further supported by simulations showing that for the same choices of parameters the model proposed in [1] may approach a non-fatal co-existing state whereas the modified model approaches a fatal state. Secondly, a model is formulated describing the impact of malignant cells becoming resistant. The model is based on the parsimonious principle and it is shown that the solutions of the model are well behaved by the establishing of a trapping region. The simulations shows how a patient may develop fatal growth of malignant cells despite continuous T-cell treatment.

Resume

Emnet for denne rapport omhandler sygdommen myeloproliferative neoplasms (MPN) som er en form for blod cancer. De præsenterede modeller vil være baseret på en model fra artiklen [1] hvor interaktionen mellem MPN og det inflammatoriske system er beskrevet. Modellen i [1] vil blive præsenteret og beskrevet. Der vil blive reflekteret over deres inklusion af et specifikt T-celle respons. Reflektionen vil i sær omhandle deres antagelse om at dødsraten for de naive T-celler er meget større end antallet af ondartede stamceller. En ny model er formuleret med et modificeret udtryk for T-celle ledet. Den modificerede model er analyseret ved brug af teorien for dynamiske systemer. Global eksistens og entydighed er garanteret ved at opstille en trapping region. En semi-analytisk undersøgelse er udført og den viser at det er muligt at modellerne vil udvise forskellig opførelse for det samme sæt af parametre. Denne undersøgelse er yderligere understøttet af simuleringer af modellerne. Dernæst er en ny model formuleret som inkluderer muligheden for at ondartede celler kan blive resistente for T-celle responset. Denne model er også analyseret ved brug af teorien for dynamiske system og de vises at modellen besidder global eksistens og entydighed. Simuleringerne viser hvordan en patient kan udvikle en fatal ondartet cellevækst på trods af forsat behandling.

Contents

Introduction

Production of blood cells take place in the bone marrow where hematopoietic stem cells proliferate into mature blood cells, namely leukocytes, erythrocytes and thrombocytes. The production of blood (haematopoiesis) is a tightly regulated process and a disturbance in this regulation process may result in fatal complications. Myeloproliferation neoplams (MPNs) is a subgroup of blood cancer where patients have an overproduction of one of the blood cell types due to presence of malignant stem cells. Malignant stem cells may cause an overproduction of cells since they have an uncontrolled proliferation. MPN predominately consists of chronic Myelogeneous Leukemia (CML), essential thrombocythemia (ET), polycythemia vera (PV) and primary myelofibrosis (PMF) [2]. CML is associated with the Philadelphia chromosome positive gen and develops over a time scale of a year. ET, PV and PMF are associated with Philadelphia chromosome negative and develop over a time scale of 10 years. These diseases may ultimately develop into acute myeloid leukemia (AML) if left untreated. AML is a progressive cancer form with a potential fatal prognosis. There are currently effective treatments available for CML. However, there are limited effective treatments available for ET, PV and PMF [1] thus this is a motivating factor for modeling these diseases.

Mathematical modeling is used to describe the dynamics of the development of MPN. Mathematical modeling is a widely used tool and it's used in several areas of science, like information and communication technology, bioengineering, financial engineering [3]. For complex systems it is often unknown how different quantities depend on each other and a strength of mathematical modeling is that for such complex systems a mathematical model may provide a detailed analysis which may reveal the important dynamics of complex systems. An example of a complex system is the development of cancerous diseases like MPNs. The human body consist of several complex systems for which we know very little about. Thus mathematical modeling have a huge potential within the area of bio-technology since it may change the current view on a physiological system or confirm/support the view. Moreover, the models allow for analysing the effect of changing parameters and thereby reduce the need for physical experiments which may be time consuming and a costly process. However, there a pit falls for mathematical modeling. The models are almost never an exact representation of the real system [3] whereby the models only represent an approximation of the true underlying dynamics of the system. The models are therefore often based on simplifying assumptions and if these do not hold, then the conclusions drawn from the models may be incorrect and misleading. Thus the models should be used for guidelines rather than as the ground truth.

In this project the mathematical models will be based on differential equations. Differential equations are often used to model biological phenomena since they arise naturally from conservation laws. Conservation laws describe the change in amount pr. time for a given quantity, i.e. they can be used to describe the dynamics of the system. The systems will be analysed using the theory of dynamical systems. A mathematical model describing the development of MPN and its coupling to the immune system is proposed in [4]. This model has been extended to include the effect of the T-cell response in [1].

1.1 Project Outline

In this project the model for modeling MPNs proposed in [1] is presented. The modeling choices in [1] will be reflected upon and in particular the equation describing the inclusion of the T-cells will be discussed. We will formulate a new model where the T-cell specific term is modified. This new model will be referred to as the modified T-cell model. Moreover, the concept of malignant cells turning resistant to the T-cell specific response will be discussed and a new model for modeling this phenomena is formulated. The models will be discussed and reflected upon in context of the current biology theory and in relation to the modeling process.

Thus the contribution of this project is mainly the two proposed models which are both based on the T-cell model in [1]

- *The Modified T-cell Model:* The term including the T-cell specific response is modified.
- *The Resistant T-cell Model:* An inclusion of a malignant stem cell line which is resistant to the T-cell specific response.

1.2 Method

The framework of the project consists of two introductory chapters, namely Chapter 2 introducing the basic biology theory and Chapter 3 describing the mathematical theory used for the analysis of the models. The models will be formulated as nonlinear ordinary differential equations and will be analysed using the theory of dynamical systems. In Chapter 3 it is assumed that the reader is familiar with the theory of linear dynamical systems. The theory presented will be concerning nonlinear dynamical theory and for which conditions we may analyse a nonlinear system by its linearization. Chapter 4 is concerning mathematical modeling. In this chapter the process of mathematical modeling is discussed and the model proposed in [1] is presented and discussed. Moreover, the two new model proposals *the modified T-cell model* and *the resistant T-cell model* are formulated and discussed. In Chapter 5 numerical experiments are made to investigate the analytic findings in Chapter 4. A discussion of the proposed models and the numerical experiments are discussed in Chapter 6 along with a discussion of the biological interpretations of the modeling and numerical experiments. Lastly, the conclusion is presented in Chapter 7.

Biological Theory

In this chapter the reader is introduced to basic biological theory describing the cell proliferation and the coupling to the immune response. Furthermore, the disease myeloproliferative neoplasms (MPNs) is introduced and it is explained how this group of diseases effect the cell proliferation.

2.1 Hematopoietic Cells

The organs of the human body are composed of a mixed of different specialized cell types. Cells are responsible for repairing and maintaining the organs and protecting the body from infections and diseases. The hematopoietic cells (blood cells) are the cells that live in the blood. There are three types of blood cells namely, erythrocytes (red blood cells), thrombocytes (platelets) and leukocytes (white blood cells) and in a healthy adult there are approximately 10^{12} erythrocytes, 10^{11} thrombocytes and 10^9 leukocytes [5]. The erythrocytes transport oxygen throughout the capillaries to provide the tissue with oxygen. The platelets are responsible for blood clotting and healing wounds and lastly the leukocytes are cells of the immune system that protects against foreign invaders like vira and bacteria [6]. All of these blood cells are produced by the hematopoietic stem cells (HSCs). HSCs live in the bone marrow niches which are local tissue micro-environments that maintain and regulate stem cells by stimulating proliferation and self-renewal. Thus the HSCs play an important role in maintaining a healthy hematopoiesis (production of blood) [7]. Hematopoiesis is a tightly regulated process and a disturbance in the hematopoisis may result in severe consequences like the development of blood cancer [8]. Based on the observations in healthy adults, the numbers of hematopoietic stem cells are approximately $2 \cdot 10^4$ [9].

2.2 Hematopoietic Stem Cells

Stem cells are distinguished from other cell types by their ability of self-renewal and proliferation into all other types of cells. Cell proliferation is rapid mitosis (cell division) thus proliferation enables a rapid increase in the number of cells. New cells can thereby be continuously generated which enables the organism to replace dead and damaged cells. Mitosis of a cell is defined by the mother cell (the cell itself) dividing into two daughter cells. For mitosis of a HSC the

daughter cell can either become a new HSC or a hematopoietic progenitor cell (HPC). An HPC is slightly more differentiated than an HSC and will eventually differentiate into a hematopoietic mature cell (HMC), which is a fully specialized cell. Hence the mitosis of an HSC has three different outcomes. Either the HSC divide by symmetric self-renewal where the stem cell divides into two new stem cells. Symmetric division where the stem cell divides into two progenitor cells. Lastly, asymmetric division where the stem cell divide into one stem cell and one progenitor cell. The three different outcomes of the HSC mitosis are illustrated in Figure 2.1. Most differentiated cells are also capable of proliferation. However, they do not possess the ablility of unlimited self-renewal and as they proliferate into mature cells they can not proliferate further [10].

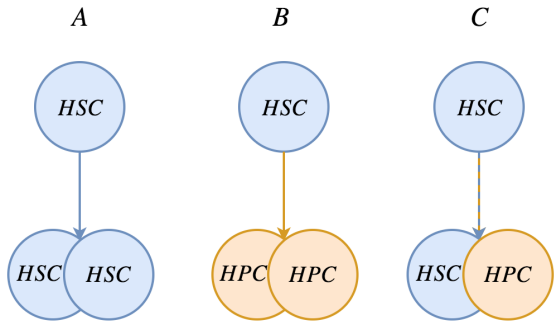

Figure 2.1: Illustration of the three outcomes of hematopoietic stem cell (HSC) mitosis. A: symmetric self-renewal producing two new HSC. B: symmetric division, producing two hematopoietic progenitor cells (HPC). C: asymmetric division, producing an HSC and an HPC.

The risk for mutations in the cell is increased during mitosis. This form for mutation is called somatic mutation [11]. Most of the somatic mutations are harmless to the organism but in some cases a sequence of mutations may lead to stem cells mutating into malignant stem cells. The malignant stem cells are like the healthy stem cells able to self-renew and proliferate. However, the malignant stem cells are characterized by an uncontrolled proliferation and self-renewal that may result in an excessive overproduction of cells. An overproduction of cells can disturb the homoeostasis which may have severe consequences for the organism. One of the possible outcome of these somatic mutations is blood cancer. Cancer is a group of diseases where the malignant cells have uncontrolled proliferation which invades or spreads to other organs [12]. In this project it is assumed that the mutation triggering cancours development occurs for the malignant stem cells and not the malignant mature cells. This theory is called *the cancer stem cell hypothesis* and is based on stem cells having several characteristics that are considered critical for the acquisition of cancer, namely the potential for unlimited cell replication, self-renewal, and long-term survival [9].

2.3 Myeloproliferation Neoplasms

A type of blood cancer is myeloproliferation neoplasms (MPN). MPN is a group of blood cancers that arise in the bone marrow. They are caused by somatic mutations that result in an overproduction of both mature and immature hematopoietic cells [13]. There are two subgroups of MPN, namely Philidelphia chromosome positive (Ph-positive) and Philidelphia chromosome negative (Ph-negative). Ph-positive is associated with the presence of a reciprocal translocation between chromosomes 9 and 22, i.e. parts of chromosome 9 and 22 have swapped resulting in an elongated chromosome 22 and a truncated chromosome 9 [8]. Ph-negative is associated with the absence of this mutation. The consequence of the presence of this mutation is a persistently enhanced tyrosine kinase (KT) activity. Tyrosine kinase is a protein that signals proliferation resulting in an uncontrolled cell division [14]. Chronic myeloid leukemia (CML) is associated with Ph-positive where the patients have an overproduction of leukocytes. The disease develops over a time line of about a year [15]. There are available treatments called tyrosine kinase inhibitors (TKI) [16] and this form of treatment has improved the prognosis for patients with CML [17].

There are three Ph-negative diseases. Namely, polycythemia vera (PV), essential thrombocythemia (ET) and primary myelofibrosis (PMF) [18]. PV denotes an overproduction of erythrocytes (red blood cells), ET denotes an overproduction of thrombocytes and primary myelofibrosis (PMF) is where excessive scar tissue forms in the bone marrow which results in a shortage of blood cells. These diseases result in an increased risk of thrombosis with cardiovascular complications, chronic inflammatory diseases and a 40% increased risk of second cancers [4]. The diseases are associated with the gene encoding Janus kinase 2 (JAK2) [18]. Almost 100% of PV and 50% of ET and PML patients have this mutation. The Ph-negative associated MPNs develop over a time line of 10 years [15] and they are considered a less progressive form for blood cancer than the Ph-positive CML. However, they may transform into acute myelogenous leukemia [19] which progresses rapidly and can be fatal if left untreated. There are limited effective treatments for the Ph-negative associated MPNs [1] which is a motivating factor for considering modeling of this group of diseases. Moreover, the equations describing the relation between healthy stem cells and malignant stem cells are similar despite the biological differences at a cellular level [1]. Thus a single model can be formulated for the development of PV, ET and PMF.

Factors like smoking, obesity and pollution are factors known to induce a chronic inflammation and thereby increases the risk of cancers [20]. Up to 20% of cancers are linked to chronic infections, where 30% can be attributed to smoking and pollutants and 20% of cancer burden is linked to obesity [21]. The inflammation level is closely connceted to the immune system and especially to the immune

surveillance which is a part of the immune system that plays a major role in the surveillance against tumors [22]. Thus in recent years research it has been argued, that the risk of developing MPNs is closely connected to the chronic inflammatory level and the immune response [4].

2.4 Immune Response

The immune response is the body's natural defence system and the cells of the immune response are specialized to fight diseases in order to ensure the survival of the organism [23]. The immune response is partly controlled by leukocytes. Leukocytes may either stimulate or suppress the self-renewal rate of the HSCs whereby the immune system may affect the hematopoisis. The immune response can be split into two parts namely the innate immune response and the adaptive immune response [23]. The innate immune response provides an immediately but non-specific response. The innate response consists of granulocytes, dendrites, macrophages and natural killer cells. These cells are responsible for the first line of defence against invaders by inducing inflammation and phagocytosis where phagocytosis is the process where foreign invaders are engulfed [24]. The adaptive immune response is activated by the innate immune response if the foreign invaders are not eliminated by the innate immune system. Thus a delay is introduced from exposure to maximal response and this delay may be up to 7 days [23]. The adaptive immune response are B-cells and T-cells also denoted lymphocytes. Lymphocytes are a subgroup of leukocytes and they represent 20% to 45% of the leukocytes blood count [25].

B-cells are involved in protecting the body against invaders by producing antibodies that detects foreign invaders and neutralize them [23]. Another important quality of the B-cells is that they have memory in the sense that if the body is exposed to the same kind of invader, the B-cells know which antibody they should produce and thereby they reduce the delay between exposure and maximal response [6] . There are several types of T-cells, in this project we will focus on naive T-cells and effector T-cells since these have been argued to have an important role in inhibbiting the development of cancer [26]. Effector T-cells are responsible for a direct defense, where they enduce death to the malignant cells. Naive T-cells are activated by Antigen Presenting Cells (APC). APC are dendrites (the most effective in activating naive T-cells), macrophages and B-cells, i.e. they are primarily activated by the innate immune response [27]. The function of naive T-cells is maturation and activation of B cells into plasma cells and memory B cells, and activation of effctor T-cells and macrophages. Furthermore, they may differentiate into effector T-cells and thereby contributing directly to the adaptive response [26]. The activation of the adaptive response is

based on intercellular communication through secretion of cytokines. Cytokines are a broad varity of small proteins that are used in intercellular communication. The cytokines play an important role in maintaining a balanced immune response and therefore the levels of cytokines can serve as markers of disease progression [23]. A motivating factor for considering the T-cell response is that gene therapy and interferon treatment focus on boosting the immune response T-cells of the patient.

As mentioned the immune system plays a major role in the surveillance against tumours and the T-cell response is active especially in the early stages of the malignant development. Patients with a low amount of immune response have a high incidence of tumours compared to patients with a normal level of immune response [22]. However, many patients develop cancer even though they have an apparently normal immune system. This indicates that the malignant cells may be able to escape the immune surveillance by becoming resistant after some time of exposure to the T-cell response [1].

Mathematical Theory

In this chapter the reader is introduced to the theory of nonlinear dynamical system. The theory of nonlinear dynamical system will be used to analyse the mathematical models and to ensure that these models are appropriate to model biological systems. It is assumed that the reader is familiar with the basic theory of linear dynamical systems and the focus of this chapter will be on the stability analysis of nonlinear systems and the global existence and uniqueness theorem. Furthermore, the concept of dimensionless analysis is introduced and lastly an instructive example is presented, illustrating the strength of dynamical system theory and dimensionless analysis.

3.1 Dynamical Systems

A dynamical system often arise from a system of differential equations. A dynamical system describes the evolution of the system over time. This quality makes dynamical system theory appropriate to model physical and biological phenomena like the dynamics of healthy and malignant cells in the MPNs.

Consider the nonlinear autonomous system of ordinary differential equations (ODEs)

$$\dot{x} = f(x),\ x \in U \subset \mathbb{R}^n,\ t \in \mathbb{R} \tag{3.1a}$$

$$x(t_0) = x_0, \tag{3.1b}$$

where $\frac{\mathrm{d}x}{\mathrm{d}t} = \dot{x}$, $f : U \subset \mathbb{R}^n \to \mathbb{R}^n$ and (3.1b) is the initial condition of the system. The solution of the initial value problem is often called the flow of the differential equation. The flow $\phi_t(x_0)$ describes the solution curve or trajectory through $x_0 \in U$.

The initial value problem in (3.1) is guaranteed to possess local existence and uniqueness if the function f is either Lipschitz continuous or a continuously differentiable function (C^1 function) [28]. Note that locally refers to that there exist a finite interval for which the solution is guaranteed to exist and is unique. Often we are interested in the *maximal interval of existence of the solution* which is the maximal interval for which we may guarentee that the solution possesses existence and uniqueness. When modeling biological systems it's desirable to ensure that the solution possesses global existence and uniqueness, since this will ensure that the solution exists for all time and is well behaved. It turns out

if f is a C^1 function and in addition the solution is bounded then the solution exists for all time. This result is summarised in Theorem 3.1 (global existence and uniqueness theorem) which is stated in [29].

Theorem 3.1 (Global Existence and Uniqueness) *Let $U \in \mathbb{R}^n$ be an open set and $f : U \subset \mathbb{R}^n$ be a C^1 function.*

(a) Given $x_0 \in U$, let (t_-, t_+) be the maximal interval of existence for $\phi_t(x_0)$. If $t_+ < \infty$ then given any compact set $C \subset U$, there is a time t_C with $0 \leq t_C \leq t_+$ such that $\phi_{t_C}(x_0) \notin C$. Similarly if If $t_- > -\infty$ there is a time t_{C-} with $t_- \leq t_{C-} \leq 0$ such that $\phi_{t_{C-}}(x_0) \notin C$.

(b) In particular if $f : \mathbb{R}^n \to \mathbb{R}^n$ and $|f(x)|$ is bounded, then the solution exists for all time.

Therefore we need only to show that the solution is bounded to ensure that the solution exists for all time. A method to show that the solution is bounded is to establish a trapping region. We will define a trapping region as a bounded region for which the flow of the differential equation is either vanishing or pointing towards the interior on the boundary of the region. This ensures that if a solution enters the region, then for all forward time the solution will stay inside this region, i.e. the solution will be bounded.

3.2 Stability of Nonlinear Systems

Dynamical systems are often analyzed by their fixed points and the stability of these since we are interested in how the system behaves when it reaches a steady state. A steady state is a state of the system for which the system is at rest and does not change for future times. Thus the steady state may be used to analyze the outcome of a disease and in this project the steady state may be used to describe if a patient will reach a healthy state where the malignant cells are eradicated, a fatal state where the malignant cells have eradicated the healthy cells or if the disease progresses to a co-existing state where the patient may live with an amount of malignant cells without fatal consequences.

A fixed point of the differential equation is defined as a point x_0 such that $f(x_0) = 0$ resulting in $\phi_t(x_0) = x_0$ for all $t \in I$. A common approach to analyse nonlinear systems and the stability of their fixed points is to apply Hartman-Grobman theorem [30].

Theorem 3.2 (Hartman-Grobman) *If x_0 is a hyperbolic fixed point for the autonomous differential equation, then there is an open set U containing x_0 and a homeomorphism H with domain U such that the orbits of the differential equation are mapped by H to orbits of the linearized system $\dot{x} = Df(x_0)(x - x_0)$ in the set U.*

Note that the linearization is simply a first order taylor expansion around x_0 since x_0 satisfies that $f(x_0) = 0$ whereby only the first order term remain. Moreover, the existence of a homeomorphism between the nonlinear and linear system ensures that they are topologically equivalent, i.e. the Hartman-Grobman theorem states that the properties of the nonlinear system are preserved by the linear system with $A = Df(x_0)$ near a hyperbolic fixed point where hyperbolic refers to the eigenvalues of the matrix A have real part different from zero. The stability of the nonlinear fixed point may therefore be described by the stability of the linear system, i.e. the stability of the fixed point x_0 is solely determined by the eigenvalues of the Jacobian at x_0. The stability of a hyperbolic fixed point may be classified by the following defintion [30].

Definition 3.3 (Stability of Hyperbolic fixed points) Let the point x_0 denote a hyperbolic fixed point for the differential equation. If all eigenvalues have negative real parts, then x_0 is called a hyperbolic sink and x_0 is a stable fixed point. If all eigenvalues have positive real parts, then x_0 is called a hyperbolic source and x_0 is an unstable fixed point. A hyperbolic fixed point x_0 that is neither a source nor a sink is called a hyperbolic saddle and x_0 is an unstable fixed point.

3.3 Dimensionless Form

Biological models often have a large number of free parameters due to complex interactions and various production rates, death rates, ect. Often it is hard to know if it's the specific choice of parameters which are important for the qualitative behaviour of the model or if it the ratios between these parameters that matters [31]. A mathematical analysis of the impact of the parameters can be performed by bringing the model into dimensionless form. Dimensionless form is a scaling of the variables such that they are dimensionless. By using this approach it's often possible to reduce the number of parameters by grouping the original parameters into clusters of parameters.

Another advantage of bringing a model into dimensionless form is that it may reveal large differences in the time scale for the variables. This is often referred to as the slow and fast dynamics of the system. If the difference in the time

scale is significant, a *quasi steady state approximation* may be applied. A quasi steady state approximation is an approximation where the equations of either the fast or slow dynamics are set to zero depending on which type of dynamic we are interested in. For modeling of blood cancer we are mainly interested in the slow dynamics since the MPNs developed over several years which is a much slower dynamic than the dynamics of the immune response. Setting a differential equation with fast dynamic to zero changes the equation into an algebraic equation which may be solved for the variable. Thereby the variable may be substituted by the found algebraic expression and the number of differential equations is reduced for each quasi steady state approximation.

3.4 Example: Predator-Prey Model

An instructive example is given to illustrate the strengths of the analysis. The chosen example is a variant of the predator-prey model

$$\dot{x} = \xi x(\gamma - x) - \lambda xy, \tag{3.2a}$$
$$\dot{y} = \lambda y(\eta x - y) - \omega y, \tag{3.2b}$$

where $x, y \geq 0$ are the variables and ξ, γ, λ, η and ω are real constants and the free parameters of the model. This system models the interaction of the population y of a predator and the population x of its prey. The model is brought into dimensionless form in attempt to reduce the number of free parameters. The dimensionless variables X, Y and T are introduced by

$$x = \bar{x}X,\ y = \bar{y}Y \text{ and } t = \bar{t}T,$$

where $\bar{x}, \bar{y}$ and $\bar{t}$ are scaling constants with the units of x, y and t. The derivative of x can be expressed in terms of the dimensionless variables by applying the chain rule

$$\dot{x} = \frac{\bar{x}}{\bar{t}}X',$$

where $X' = \frac{\mathrm{d}}{\mathrm{d}T}X$ and by the same argument we may write the derivative of y in terms of the dimensionless variables as

$$\dot{y} = \frac{\bar{y}}{\bar{t}}Y'.$$

The aim is now to choose the scaling constants such that the number of free parameters is reduced. Change of variables into dimensionless variables in (3.2) yields

$$X' = \bar{t}\left(\xi X(\gamma - \bar{x}X) - \lambda X\bar{y}Y\right),$$
$$Y' = \bar{t}\left(\lambda Y(\eta\bar{x}X - \bar{y}Y) - \omega Y\right).$$

Note that the scaling constants may be chosen in several different ways resulting in different reduced systems. However, the qualitative behavior of the different possible models will remain the same. By choosing the scaling constants as

$$\bar{x} = \gamma,\ \bar{y} = \eta\gamma \text{ and } \bar{t} = \frac{1}{\lambda\eta\gamma},$$

the following reduced system is obtained

$$X' = \alpha X(1 - X) - XY, \tag{3.3a}$$
$$Y' = Y(X - Y) - \beta Y, \tag{3.3b}$$

where $\alpha = \frac{\xi}{\lambda\eta}$ and $\beta = \frac{\omega}{\lambda\eta\gamma}$. Hence the number of free parameters are reduced from 5 to 2. This allows analysis to be carried out for the simpler system with only two free parameters. For simplicity the capital letters are discarded for the remainder of the analysis. Furthermore, the parameters are chosen to be $\alpha = 1$ and $\beta = \frac{1}{2}$.

The predator-prey model is nonlinear with $f \in C^1$ since the function f is a polynomial. Thus the dynamics of the system near hyperbolic fixed points may be analyzed by the eigenvalues of the Jacobian by Theorem 3.2. The fixed points for (3.3) are

$$(0,0)\,, \left(0, -\frac{1}{2}\right), (1,0)\,, \text{ and } \left(\frac{3}{4}, \frac{1}{4}\right),$$

but only the fixed points in the nonnegative orthant will be analyzed. The Jacobian of the system is

$$Df(x_0, y_0) = \begin{bmatrix} 1 - 2x_0 - y_0 & -x_0 \\ y_0 & x_0 - 2y_0 - \frac{1}{2} \end{bmatrix}.$$

By inserting the three nonnegative fixed points into the Jacobian and computing the eigenvalues the stability of the fixed point can be found by applying Theorem 3.3. The analysis shows that the fixed points at $(0,0)$ and $(1,0)$ are hyperbolic with eigenvalues of opposite signs thus they are hyperbolic saddle points. At $\left(\frac{3}{4}, \frac{1}{4}\right)$ both eigenvalues have negative real part and thus the fixed point may be classified as a hyperbolic sink. The phase portrait of (3.3) is shown in Figure 3.1. The phase portrait illustrates how important the fixed points and their stability are for the dynamics of the system since all trajectories are drawn towards the stable fixed point at $\left(\frac{3}{4}, \frac{1}{4}\right)$.

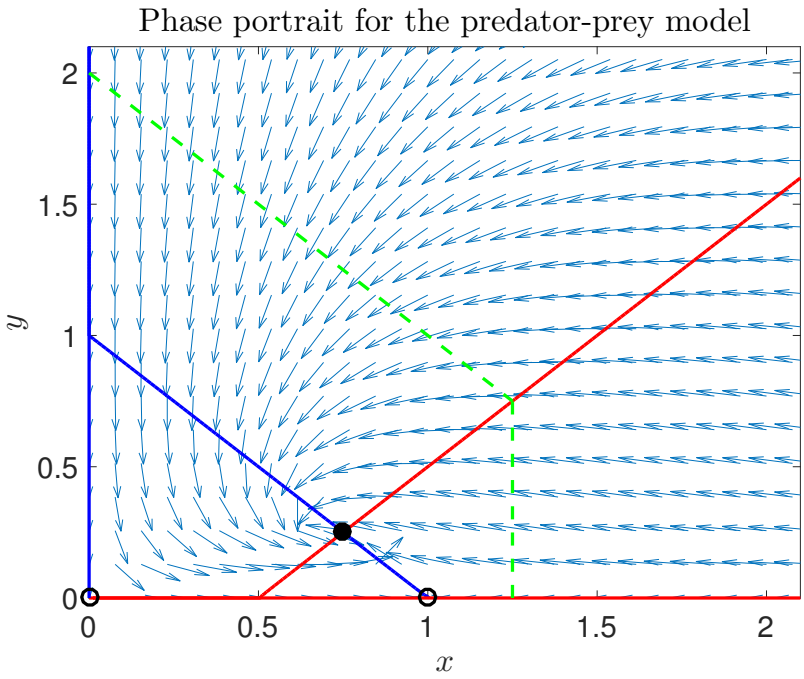

Figure 3.1: Phase portrait for the predator-prey model in (3.3) with the parameter choice $\alpha = 1$ and $\beta = \frac{1}{2}$. The figure depicts the nullclines, fixed points and a trapping region. The stability of the fixed points are indicated by the type of circle. A full circle indicates a stable fixed point whereas an open circle indicates an unstable fixed point. The blue lines correspond to the x-nullclines, the red lines correspond to the y-nullclines. The dashed green line indicates a trapping region found by connecting the line $y = b - x$, the vertical line passing through $(x, y) = (\frac{1}{2}b + \frac{1}{4}, \frac{1}{2}b - \frac{1}{4})$, the x-axis and the y-axis for the specific choice of $b = 2$.

The aim is now to establish the existence of a trapping region. Based on the model in (3.3) it can be seen that the y-axis is a nullcline for x and the x-axis is a nullcline for y. A x-nullcline is a set of points in the phase plane such that $\dot{x} = 0$. Thus if the solution starts in the nonnegative orthant it will remain there for all time due to existence and uniqueness of the solution. Let $b > \frac{3}{2}$ and consider the line

$$y = b - x.$$

On this line, the flow satisfies that

$$\begin{aligned} \dot{x} &= x(1-x) - x(b-x) = x(1-b) < 0, && \text{for } x > 0, \\ \dot{y} &= y(b-y-y) - \frac{1}{2}y = y\left(b - \frac{1}{2} - 2y\right) < 0, && \text{for } y > \frac{1}{2}b - \frac{1}{4}. \end{aligned}$$

Now consider the vertical line passing through $(x, y) = (\frac{1}{2}b + \frac{1}{4}, \frac{1}{2}b - \frac{1}{4})$. On this line the flow satisfies that

$$\begin{aligned} \dot{x} &= \left(\frac{1}{2}b + \frac{1}{4}\right)\left(1 - \left(\frac{1}{2}b + \frac{1}{4}\right)\right) - \left(\frac{1}{2}b + \frac{1}{4}\right) y \\ &\leq \left(\frac{1}{2}b + \frac{1}{4}\right)\left(1 - \left(\frac{1}{2}b + \frac{1}{4}\right)\right) < 0, \end{aligned}$$

since $b > \frac{3}{2}$. Thus a trapping region can be established by connecting the x-axis, y-axis, $y = b - x$ and $x = \frac{1}{2}b + \frac{1}{4}$ for $b > \frac{3}{2}$. Thus global existence and uniqueness may be guaranteed by Theorem 3.1 for the dimensionless predator-prey model in (3.3). Moreover, the established trapping region also guarantees global existence and uniqueness for the predator-prey model in (3.2) since the dynamics of this two systems are equivalent. The trapping region for the predator-prey model is depicted in Figure 3.1 for the specific choice of $b = 2$.

The Mathematical Models

In this chapter the reader is introduced to the concept of mathematical modeling where the strengths and weaknesses of mathematical modeling will be reflected upon. The models presented in [4] and [1] will be introduced and explained in details. The inclusion of T-cells in [1] will be reflected upon and a more complicated model for the T-cell response is proposed and analysed. Moreover, the concept of the malignant cells turning resistant to the T-cell response is included in the model in [1].

4.1 Mathematical Modeling

Mathematical modeling is becoming increasingly acknowledged within areas of science, like information and communication technology, bio-engineering and financial engineering [3]. Physical and biological systems may be expressed in terms of force and mass balances, according to the laws of conservation. The conservation laws result in mathematical equations which may constitute a mathematical model. A mathematical model is a theoretical representation of a physical system and often it can be used for simulating highly complex systems. A strength of mathematical modeling is that mathematics is a concise language that may grant insight into the dynamics of the system and thereby obtaining information about how the dynamics depend on the parameters and which of these that are most important for the evolution of the system [31]. This insight may reduce the need for physical experiments which are often time consuming and costly. Thus mathematical modeling provides potential advantage to industries [3].

The process of mathematical modeling may be described by the modeling cycle. A simple illustration of the modeling cycle is shown in Figure 4.1. A current preption of a phenomena may be formulated as a mathematcal model. The model can then be analyzed using mathematical tools. The analysis of the model and the results may change this perception of the reality by potentially granting new insight for the modeled phenomena. Thus often models are formulated in several iterations due to new insight obtained in one or several of the stages of modeling. The modeling process for this project may be interpreted as iterations of the modeling cycle. Based on the current model in [1], possible extensions of the model is proposed based on a new perception of the reality. The proposed extended models may then again give rise to considering other changes or investigating the chosen phenomena further whereby the cycle keeps on iterating.

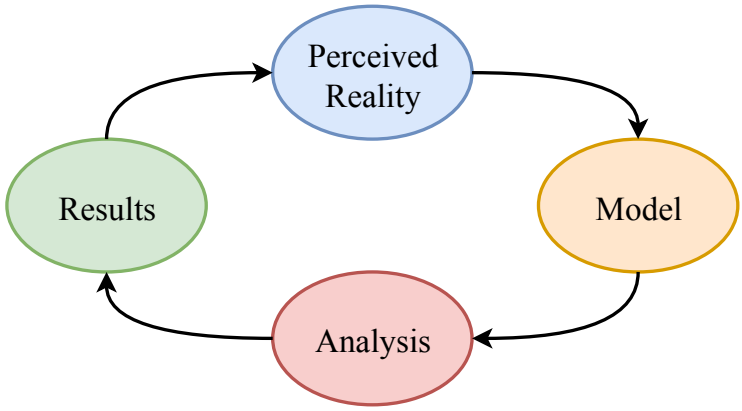

Figure 4.1: Illustration of the modeling cycle. The modeling cycle is an iterative process and the models may adjusted through several iterations due to new obtained knowledge and/or changed perception of the reality.

However, there are limitations to mathematical modeling. For complex systems, the model are rarely capable of capturing the total complexity of the dynamics whereby the model only present a simplified model of the true underlying dynamics, i.e. the mathematical model becomes an idealization of the studied phenomenon [31]. Thus the models are often based on simplifying assumptions and if these do not hold, then the conclusions drawn from the model may be incorrect and misleading. Moreover, even if every dynamic of a complicated system were included we would likely end up with an extremely complex model with lots of parameters such that the analysis may become very difficult and not revealing the important factors for the dynamics. Thus mathematical modeling is a challenging discipline where the aim is to include the features with the greatest influence and omit the rest. This idea is also formulated as parsimonious principle. Parsimonious principle states that we aim to choose the simplest model that fits the data, i.e. only the essential dynamics are included in the model and everything else are excluded. Often it is not trivial which features to include and which to omit or which assumptions that are appropriate for the system. Thus the best model is often found by iterating through the modeling cycle in Figure 4.1.

In this project the mathematical models will be based on compartment modeling. Compartment modeling assumes that each compartment is homogeneous and is based on conservation laws. Hence the model allows material to either flow from one compartment to another, being added through a source, or being removed through a sink [32]. Compartment modeling is chosen for the model of MPNs since we are not interested in the events for a single cell but in the overall

dynamic between the healthy cells and the malignant. A ordinary differential equation will be formulated for each compartment based on conservation laws, i.e.

$$\text{Accumulated} = \text{Generated} - \text{Eliminated},$$

where accumulated refers to the change in amount of a compartment pr. time, generated refers to the rate of generation times the generating source and eliminated refers to the rate of elimination times the current amount in the compartment.

4.2 The Basic Model

This project will be based on the model proposed in [4] which will be refered to as the basic model. Moreover, the model with the extension to include T-cell response as proposed in [1] will be referred to as the T-cell model. First an outline of the basic model is presented and then the T-cell response is introduced. For this project a compartment will refer to the amount of a specific type of cell, healthy stem cells (HSC), healthy mature cells (HMC), malignant stem cells (MSC) or malignant mature cells (MMC) or the level of infection (immune response). An ordinary differential equation is formulated for each compartment based on the conservation principle. The basic model is illustrated in Figure 4.2. The model consists of six compartments where x_0 denotes the amount of HSC, x_1 denotes the amount of HMC, y_0 denotes the amount of the MSC, y_1 denotes the amount of MMC, s denotes the inflammatory level, i.e. the immune response and a is the amount of dead cells.

The generated amount of HSC per time, x_0 depends on the self-renewal rate, r_x, the inhibitory niche feedback described by the function φ_x and the inflammatory level s and the current amount of x_0. The immune response stimulates HSC self-renewal due to potential high necrosis whereas the inhibitory niche feedback inhibits the self-renewal. Thus the function φ is chosen to be a decreasing function of x_0 and y_0. The eliminated amount of HSC per time is described by the death rate of x_0, denoted d_{x_0} and the proliferation rate, a_x. In addition, there is a chance for a HSC to mutate into a MSC which is described by the mutation rate, r_m. The probability of mutating is further increased by a high inflammatory level and the mutation rate therefore also depends on the variable s, thus this the mutating term is modeled as a second order reaction kinetics. Formulating this in the language of mathematics yields the following differential equation

$$\dot{x}_0 = (r_x\varphi_x(x_0, y_0)s - d_{x_0} - a_x)x_0 - r_m s x_0,$$

where $\dot{x}_0 = \frac{\mathrm{d}}{\mathrm{d}t}x_0$. The same considerations can be applied to the accumulation of MSC, y_0. However, the difference is that the probability of mutation generates

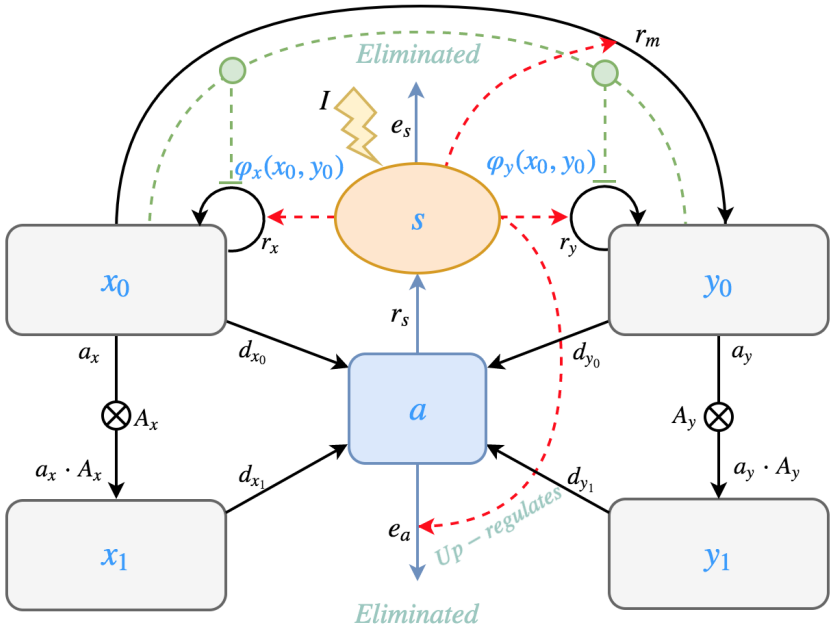

Figure 4.2: The conceptual model describes the dynamic between the healthy cells and the malignant cells and is based on the model presented in [4]. The light grey boxes are the cell compartments where x_0 denotes the number of healthy stem cells, x_1 denotes the healthy mature cells, y_0 that of maglinant stem cells, and y_1 the number of malignant mature cells. The light blue compartment a denotes the amount of dead cells and the light orange compartment denoted s describes the inflammatory level. The black arrows indicate a flow from one compartment to another, red stipulated arrows illustrates regulation of the cytokines and the green stipulated line indicates the inhibitory effect in the bone marrow niche.

MSC instead of eliminating MSC. Hence the accumulation of MSCs pr. time can be described by

$$\dot{y_0} = (r_y \varphi_y(x_0, y_0)s - d_{y_0} - a_y)y_0 + r_m s x_0.$$

The accumulation for HMC, x_1 can be described by the amount of HSC that proliferate into mature cells. HSC proliferates into progenitor cells with rate a_x. However, in this model we consider the mature cell and not the progenitor cells. Thus the generation rate of mature cells is found by multiplying the rate of proliferation of the HSC by a constant, A_x which describes the total amount of generated mature cells pr. stem cell proliferation, i.e the generated amount of HMC is given by the rate $a_x A_x$. The elimination of HMC is given by the

death rate d_{x_1} and the differential equation for x_1 is therefore given by

$$\dot{x}_1 = a_x A_x x_0 - d_{x_1} x_1.$$

Similarly the following differential equation is obtained for the MMCs y_1,

$$\dot{y}_1 = a_y A_y y_0 - d_{y_1} y_1.$$

The generated amount of dead cells is governed by the total amount of dead cells from the four light grey compartments in Figure 4.2. The elimination of dead cells is assumed to depend on the inflammatory level and the total amount of dead cells as second order reaction kinetics. Thereby the following differential equation is obtained for the accumulation of dead cells

$$\dot{a} = d_{x_0} x_0 + d_{y_0} y_0 + d_{x_1} x_1 + d_{y_1} y_1 - e_a a s.$$

Lastly, the inflammatory level is govern by

$$\dot{s} = r_s a - e_s s + I,$$

where r_s is the rate for which the number of dead cells up regulates the immune response, e_s is the elimination rate for the inflammatory level and I is an external stimuli of the immune response such as smoking, pollution or obesity. Hence we end up with a system of coupled nonlinear differential equations

$$\dot{x}_0 = (r_x \varphi_x(x_0, y_0) s - d_{x_0} - a_x) x_0 - r_m s x_0, \tag{4.1a}$$
$$\dot{y}_0 = (r_y \varphi_y(x_0, y_0) s - d_{y_0} - a_y) y_0 + r_m s x_0, \tag{4.1b}$$
$$\dot{x}_1 = a_x A_x x_0 - d_{x_1} x_1, \tag{4.1c}$$
$$\dot{y}_1 = a_y A_y y_0 - d_{y_1} y_1, \tag{4.1d}$$
$$\dot{a} = d_{x_0} x_0 + d_{y_0} y_0 + d_{x_1} x_1 + d_{y_1} y_1 - e_a s a, \tag{4.1e}$$
$$\dot{s} = r_s a - e_s s + I. \tag{4.1f}$$

The φ functions are chosen as

$$\varphi_x(x_0, y_0) = \frac{1}{1 + (c_{xx} x_0 + c_{xy} y_0)},$$
$$\varphi_y(x_0, y_0) = \frac{1}{1 + (c_{yx} x_0 + c_{yy} y_0)}.$$

where it is assumed that $c_{yy} \leq c_{yx} \leq c_{xy} \leq c_{xx}$ such that the malignant cells are less sensitive to inhibitive niche feedback than the healthy hematopoietic cells. Other choices of function may be considered. However, the investigations in [1] showed no qualitative difference in the results and thus this function will be used throughout the project. Furthermore, for the rest of the project it is assumed that a mutation sequence has occurred resulting in $y_0 = 1$ at $t = 0$

and that $r_m = 0$ for all time which is based on the assumption that the first malignant mutation will drive the dynamics of the malignant cells which is the assumption proposed in [1]. The default parameters for the basic model in (4.1) which will be used for simulation throughout the project are listed in Table 4.1.

Parameter	Value	Unit
r_x	$8.7 \cdot 10^{-4}$	day^{-1}
r_y	$1.3 \cdot 10^{-3}$	day^{-1}
a_x	$1.1 \cdot 10^{-5}$	day^{-1}
a_y	$1.1 \cdot 10^{-5}$	day^{-1}
A_x	$4.7 \cdot 10^{13}$	-
A_y	$4.7 \cdot 10^{13}$	-
d_{x_0}	$2 \cdot 10^{-3}$	day^{-1}
d_{y_0}	$2 \cdot 10^{-3}$	day^{-1}
d_{x_1}	129	day^{-1}
d_{y_1}	129	day^{-1}
c_{xx}	$5.6 \cdot 10^{-5}$	-
c_{xy}	$5.4 \cdot 10^{-5}$	-
c_{yx}	$5.2 \cdot 10^{-5}$	-
c_{yy}	$5.0 \cdot 10^{-5}$	-
e_s	2	day^{-1}
e_a	$2 \cdot 10^9$	day^{-1}
r_s	$3 \cdot 10^{-4}$	day^{-1}
I	7	day^{-1}

Table 4.1: Default parameters for the model (4.1).

All the interactions expect the ϕ function are modeled as either 1. order or 2. order terms. This approach is often used to model cell interaction due to the great advantage of simplifying the mathematical analysis. The basic model is based on a model for CML presented in [9] where they argue that the cancerous development is driven by the malignant stem cells. Moreover, they argue that including a more complex negative-feedback system did not lead to significant differences from the conclusions derived from this simple model whereby the simpler model was preferred by the parsimonious principle.

4.3 The T-cell Model

In [1] the basic model presented in (4.1) is extended to include the effect of the T-cells specific response. This inclusion is inspired by [33] where T-cell response is argued to have a significant impact on the cancerous development for CML. The extension considers the impact of naive and effector T-cells on the death rates of the malignant cells. It is assumed that the naive T-cells T_n are produced by a constant rate, p_n and and that the naive T-cells may transform into effector T-cells, T_e proportional with the amount of malignant cells y by the constant rate k_n. Moreover it is assumed that the dynamic is driven by the stem cell dynamics, i.e. the important impact from the T-cell response comes from the elimination of malignant stem cells. Thus the T-cell response is only considered explicitly in the equation governing the accumulation of malignant stem cells and it is assumed that this elimination is a second order reaction kinetics with rate γ_{y_0}. The new expression for y_0 taking the T-cell response explicitly into account is given by

$$\dot{y}_0 = (r_y \varphi_y(x_0, y_0)s - d_{y_0} - \gamma_{y_0} T_e - a_y)y_0 \tag{4.2}$$

The naive T-cell are eliminated by a constant rate η due to apoptosis and hence the differential equation for the accumulation of naive T-cells is given by

$$\dot{T}_n = p_n - k_n T_n(y_0 + \eta). \tag{4.3}$$

The naive T-cells turns into effector T-cells T_e when exposed to malignant stem cells with rate α_n. They are eliminated by a constant rate γ_e due to apoptosis. Thus the accumulation of effector T-cells may be governed by the differential equation

$$\dot{T}_e = \alpha_n k_n T_n y_0 - \gamma_e T_e. \tag{4.4}$$

Note that the equations in (4.3) and (4.4) are inspired by the equations proposed in [33] but are simpler since they consists of polynomial equations whereas the equations proposed by [33] includes Michaelis–Menten terms based on the assumption that effector T-cells encounter MPN cells in the lymph and arguing that there are limitations of the immune response, due to the large numbers of APC presenting malignant antigen which saturate the lymph, but the relatively few specific naive T cells, i.e.

$$k_n T_n \frac{y}{y + \xi}.$$

Thus in the T-cell model proposed in [1] then these modifications may be based on the assumption that there is no limiting effect of the encounter in the lymph and that the encounter between naive T-cells and malignant stem cells occur in a manner similar to how the encounter would be in the blood stream. Another

interpretation could be that the T-cell model includes a linearization of the Michalis-Mentel term since

$$k_n T_n \frac{y}{y+\xi} \approx \tilde{k}_n T_n y \quad \text{for} \quad \xi \gg y,$$

with $\tilde{k}_n = \frac{k_n}{\xi}$. The strength of the simpler term is that it simplifies the analysis due to it being a simple second order term and thereby simplifying the quasi steady state approximation.

4.3.1 Quasi Steady State Approximation

Based on the biology response the T-cell response is assumed fast compared to the slower development of the MPNs. Hence a quasi steady state approximation may be applied to (4.3) and (4.4) in order to reduce the number of differential equations, i.e. we assume that $\dot{T}_e \approx 0$ and $\dot{T}_n \approx 0$. From the first approximation we get that T_n can be approximated by

$$T_n \approx \frac{p_n}{k_n(y_0+\eta)},$$

and similarly by substituting the found expression for T_n into the second approximation we get

$$T_e \approx \frac{\alpha_n p_n}{\gamma_e} \frac{y_0}{y_0+\eta}. \tag{4.5}$$

Thus the effector T-cells may be described by a Michalis Mentel term, indicating that the amount of effector T-cells have a saturation and does not increase proportional to the amount of malignant stem cells. Thus this term may provide the model with the saturating effect of the T-cell response which was ommited in the differential equations for T_n and T_e. However, in [1] it is assumed that the death rate of naive T-cells is significantly larger than the amount of malignant stem cells, i.e. it is assumed that $\eta \gg y_0$, resulting in the linear approximation

$$T_e \approx \frac{\alpha_n p_n}{\gamma_e \eta} y_0. \tag{4.6}$$

This assumption simplifies the expression for the effector T-cells such that they are simply proportional to the amount of malignant stem cells whereby there are no saturation of the T-cell specific response. The death rate of naive T-cells η is suggested to be $\eta \approx 0.04\,\text{day}^{-1}$ in [34] and based on this estimate it does not seem likely that the approximation hold. Hence the consequences of this approximation is a subject for further investigation.

As mentioned the effect of T-cells only changes the death rate of the malignant stem cells since it was assumed that the important impact of the T-cell response

was the impact on the death of malignant stem cells. Thus only (4.1b) and (4.1e) have to be modified whereas the other equations in (4.1) remain unchanged. The expression found in (4.6) is then substituted into (4.2) and the T-cell model then becomes

$$\dot{x}_0 = (r_x\varphi_x(x_0, y_0)s - d_{x_0} - a_x)x_0, \tag{4.7a}$$
$$\dot{y}_0 = (r_y\varphi_y(x_0, y_0)s - d_{y_0} - \tilde{d}_{y_0}y_0 - a_y)y_0, \tag{4.7b}$$
$$\dot{x}_1 = a_x A_x x_0 - d_{x_1}x_1, \tag{4.7c}$$
$$\dot{y}_1 = a_y A_y y_0 - d_{y_1}y_1, \tag{4.7d}$$
$$\dot{a} = d_{x_0}x_0 + (d_{y_0} + \tilde{d}_{y_0}y_0)y_0 + d_{x_1}x_1 + d_{y_1}y_1 - e_a sa, \tag{4.7e}$$
$$\dot{s} = r_s a - e_s s + I, \tag{4.7f}$$

where $\tilde{d}_{y_0} = \gamma_{y_0}\frac{\alpha_n p_n}{\gamma_e \eta}$ is the new parameter describing the effect of the T-cell response.

The model has a high number of free parameters and thus the model is converted into dimensionless form to reduce the number of parameters. The number of free parameters are reduced by grouping the original parameters into clusters of parameters. These clusters of the original parameters become the dimensionless parameters.

4.3.2 Dimensionless Form

This strategy is proposed in [1]. The equations in (4.7) are put into dimensionless form by using the same strategy as in the instructive example for the predator-prey model in (3.3). Thus the variables are scaled by constants having the same unit as the variable if any. The dimensionless variables are denoted by capital letters and the scaling constants are denoted by the same symbols as the corresponding original variable with a bar, an example is for the HSC compartment where x_0 can be expressed by $x_0 = \bar{x}_0 X_0$ whereas the derivative can be expressed

$$\dot{x}_0 = \frac{\bar{x}_0}{\bar{t}} X_0',$$

with $X_0' = \frac{\mathrm{d}}{\mathrm{d}T}X_0$. Hence the model in (4.7) is equivalent with

$$
\begin{aligned}
X_0' &= \bar{t}\left(\bar{s}r_x\frac{S}{1+(c_{xx}\bar{x}_0X_0+c_{xy}\bar{y}_0Y_0)} - d_{x_0} - a_x\right)X_0,\\
Y_0' &= \bar{t}\left(\bar{s}r_y\frac{S}{1+(c_{yx}\bar{x}_0X_0+c_{yy}\bar{y}_0Y_0)} - \hat{d}_{y_0}(Y_0) - a_y\right)Y_0,\\
X_1' &= \bar{t}\left(\frac{\bar{x}_0}{\bar{x}_1}a_xA_xX_0 - d_{x_1}X_1\right),\\
Y_1' &= \bar{t}\left(\frac{\bar{y}_0}{\bar{y}_1}a_yA_yY_0 - d_{y_1}Y_1\right),\\
A' &= \bar{t}\left(d_{x_0}\frac{\bar{x}_0}{\bar{a}}X_0 + \hat{d}_{y_0}(Y_0)\frac{\bar{y}_0}{\bar{a}}Y_0 + d_{x_1}\frac{\bar{x}_1}{\bar{a}}X_1 + d_{y_1}\frac{\bar{y}_1}{\bar{a}}Y_1 - e_a\bar{s}SA\right),\\
S' &= \bar{t}\left(r_s\frac{\bar{a}}{\bar{s}}A - e_sS + \frac{I}{\bar{s}}\right),
\end{aligned}
$$

where $\hat{d}_{y_0}(Y_0) = d_{y_0} + \tilde{d}_{y_0}\bar{y}_0Y_0$. The dimensionless model is then simplified by choosing the scaling constants such that the parameters are clustered into the new dimensionless parameters. The choice of scaling is chosen as proposed in [1], i.e.

$$
\begin{aligned}
\bar{s} &= \frac{d_{x_0}+a_x}{r_x},\\
\bar{a} &= \frac{e_s}{r_s}\bar{s},\\
\bar{x}_0 &= \frac{1}{c_{xx}},\\
\bar{x}_1 &= \frac{a_xA_x}{c_{xx}d_{x_1}},\\
\bar{y}_0 &= \frac{1}{c_{yy}},\\
\bar{y}_1 &= \frac{a_yA_y}{c_{yy}d_{y_1}},\\
\bar{t} &= \frac{1}{d_{x_0}+a_x}.
\end{aligned}
$$

Inserting the scaling constants into the dimensionless model yields

$$\dot{X}_0 = \left(\frac{S}{1 + (X_0 + \frac{c_{xy}}{c_{yy}} Y_0)} - 1 \right) X_0, \tag{4.8a}$$

$$\dot{Y}_0 = \left(\frac{r_y}{r_x} \frac{S}{1 + (\frac{c_{yx}}{c_{yy}} X_0 + Y_0)} - \frac{\hat{d}_{y_0}(Y_0) + a_y}{d_{x_0} + a_x} \right) Y_0, \tag{4.8b}$$

$$\varepsilon_1 X_1' = X_0 - X_1, \tag{4.8c}$$

$$\varepsilon_1 Y_1' = \frac{d_{y_1}}{d_{x_1}} (Y_0 - Y_1), \tag{4.8d}$$

$$\varepsilon_2 S' = A - S + \frac{I}{e_s \bar{s}}, \tag{4.8e}$$

$$\varepsilon_2 \varepsilon_3 A' = b_{x_0} X_0 + b_{y_0}(Y_0) Y_0 + b_{x_1} X_1 + b_{y_1} Y_1 - AS, \tag{4.8f}$$

where $\varepsilon_1 = \frac{r_x}{d_{x_1}} \bar{s}$, $\varepsilon_2 = \frac{r_x}{e_s} \bar{s}$, $\varepsilon_3 = \frac{e_s}{e_a} \bar{s}$, $b_{x_0} = d_{x_0} \frac{\bar{x}_0 \bar{t}}{\bar{s}\bar{a}} \frac{d_{x_0} + a_x}{e_a}$, $b_{y_1} = d_{y_1} \frac{\bar{y}_1 \bar{t}}{\bar{s}\bar{a}} \frac{d_{x_0} + a_x}{e_a}$, $b_{y_0}(Y_0) = \hat{d}_{y_0}(Y_0) \frac{\bar{y}_0 \bar{t}}{\bar{s}\bar{a}} \frac{d_{x_0} + a_x}{e_a}$. The magnitudes of the parameters are shown in Table 4.2.

Parameter	ε_1	ε_2	ε_3	b_{x_0}	b_{x_1}	b_{y_0}	b_{y_1}
Magnitude	10^{-5}	10^{-3}	10^{-10}	10^{-13}	10^{-1}	10^{-13}	10^{-1}

Table 4.2: Magnitudes of the parameters in the dimensionless T-cell model in (4.8).

This formulation of the model reveals that the processes evolve on different time scales and that the system has slow and fast dynamics. This change in time scale is due to the multiplication of the ε parameters on (4.8c)-(4.8f). We are mostly interested in the slow dynamics of the system since these are the dynamics describing the development of the MPNs thus we may consider the slow manifold approximation by studying the equations in the limit of $\varepsilon \to 0$ and thereby obtaining a system of two equations. In the limit of $\varepsilon \to 0$ the left hand side vanishes and the following algebraic equations are obtained from equation (4.8c)-(4.8d)

$$0 = X_0 - X_1, \tag{4.9a}$$

$$0 = Y_0 - Y_1, \tag{4.9b}$$

$$0 = A - S + \frac{I}{e_s \bar{s}}, \tag{4.9c}$$

$$0 = b_{x_0} X_0 + b_{y_0}(Y_0) Y_0 + b_{x_1} X_1 + b_{y_1} Y_1 - AS. \tag{4.9d}$$

These four equations can be solved for X_1, Y_1, A and S. The first two are simple

and are given by

$$X_1 = X_0,$$
$$Y_1 = Y_0.$$

Substituting these expressions into (4.9d) gives

$$0 = b_{x_0}X_0 + b_{y_0}(Y_0)Y_0 + b_{x_1}X_0 + b_{y_1}Y_0 - AS.$$

Introducing new parameters as $2B_x = b_{x_0} + b_{x_1}$ and $2B_y = b_{y_0}(Y_0) + b_{y_1}$, then the equation can be expressed

$$0 = 2B_xX_0 + 2B_yY_0 - AS. \tag{4.10}$$

Note that the difference in magnitude is large for b_{x_0} and b_{x_1} since $b_{x_1} \sim 10^{-1}$, $b_{x_0} \sim 10^{-13}$ and Y_0 is scaled such that it will not attain values much larger than 1, thus we may choose to approximate $2B_x$ by $2B_x \approx b_{x_1}$. The same approximation is made for $2B_y$, i.e. $2B_y \approx b_{y_1}$. Note that this approximation makes B_y independent of Y_0 which simplifies the expression and results in that the only change by adding T-cell response appears in equation (4.8b). Solving the equations (4.9c) and (4.10) give

$$S = J \pm \sqrt{J^2 + 2B_xX_0 + 2B_yY_0},$$
$$A = \pm\sqrt{J^2 + 2B_xX_0 + 2B_yY_0},$$

where $J = \frac{I}{2e_s\bar{s}}$. However, only the positive solutions are considered to be in accordance with the biological theory thus A and S are found to be

$$S = J + \sqrt{J^2 + 2B_xX_0 + 2B_yY_0}, \tag{4.11a}$$
$$A = \sqrt{J^2 + 2B_xX_0 + 2B_yY_0}, \tag{4.11b}$$

By inserting (4.11a) into (4.8a) and (4.11b) into (4.8b), the model (4.8) can be approximated by the following reduced model

$$X_0' = \left(\frac{J + \sqrt{J^2 + 2B_xX_0 + 2B_yY_0}}{1 + X_0 + C_yY_0} - 1\right)X_0, \tag{4.12a}$$
$$Y_0' = \left(R\frac{J + \sqrt{J^2 + 2B_xX_0 + 2B_yY_0}}{1 + C_xX_0 + Y_0} - D_0 - D_1Y_0\right)Y_0, \tag{4.12b}$$

where $R = \frac{r_y}{r_x}$, $C_x = \frac{c_{xy}}{c_{yy}}$, $C_y = \frac{c_{yx}}{c_{xx}}$, $D_0 = \frac{d_{y_0}+a_x}{d_{x_0}+a_x}$ and $D_1 = \frac{\tilde{d}_{y_0}\bar{y}_0}{d_{x_0}+a_x}$. Thereby the model in (4.8) has been reduced to a system of two equations and the number of parameters have been reduced from 19 to 8. The default dimensionless

parameter choice is shown in Table 4.3. These are based the default parameters presented in Table 4.1 and they are the parameters used in the simulations unless stated otherwise. Note that the clustering of the parameters reveals which ratios of parameters that are important for the development of the MPNs. R describes the ratio of self-renewal, since $R > 1$ this reflects that the MSCs have a higher rate of self-renewal than the HSCs. J describes the dimensionless inflammatory stimuli, D_0 describes the T-cell independent death rate of Y_0 whereas D_1 describes the T-cell dependent death rate of Y_0. C_x and C_y express the inhibitory niche effect favouring the self-renewal of malignant stem cells whereas B_x and B_y describe the dimensionless death rates.

Parameter	R	J	D_0	D_1	C_x	C_y	B_x	B_y
Value	1.49	0.76	1.00	0.10	0.93	1.08	0.06	0.07

Table 4.3: Default dimensionless parameter values for the T-cell model in (4.12).

In the following analysis and simulations we will mainly consider the effect of changing the parameter describing the T-cell dependent death rate of Y_0 since the later proposed changes for the T-cell model concern the effect of this term. However, the T-cell model proposed in [1] reveals interesting results and constitutes to the idea that chronic inflammation may trigger and drive blood cancer whereby the parameter J describing dimensionless inflammatory stimuli is shown to guarantee the existing of a leukemic steady state if chosen large enough [1]. Thus the T-cell model supports the theory that cancerous diseases may be driven by chronic inflammation as proposed in [21].

In Figure 4.3 simulations with the full model (4.8) and the reduced model (4.12) are shown. The simulations show how the MPNs develop for different choices of D_1, i.e. simulations for different levels of T-cell dependent response. The figure shows that the reduced model is in accordance with the full model. Moreover the simulations show that if a patient has the standard parameters in Table 4.3, then an increase in the T-cell response may change the development of MPN from a fatal scenario to a scenario where the patient may live with the disease due to a co-existing steady state which is verified by the corresponding phase portraits for the reduced T-cell model in Figure 4.4. In Figure 4.4 a full circle indicates that all the eigenvalues have negative real part resulting in a stable fixed point and an open circle indicates that there is at least one eigenvalue with positive real part resulting in an unstable fixed point. The fixed points are classified as either trivial, hematopoietic, leukemic or co-existing where they are defined as

- **Trivial fixed point:** having $X_0 = 0$ and $Y_0 = 0$
- **Hematopoietic fixed point:** having $X_0 > 0$ and $Y_0 = 0$
- **Leukemic fixed point:** having $X_0 = 0$ and $Y_0 > 0$
- **Co-existing fixed point:** having $X_0 > 0$ and $Y_0 > 0$

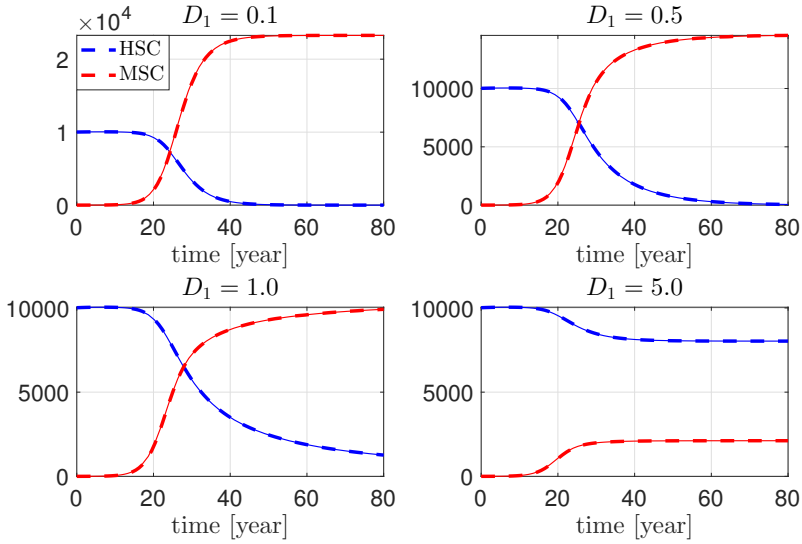

Figure 4.3: Simulations of the full dimensionless T-cell model in (4.8) and the reduced dimensionless T-cell model in (4.12) (stipulated lines) proposed in [1]. The blue lines are the healthy HSC and the red are the malignant MSC. The simulations show that the reduced model is in accordance with the full model.

The phase portraits show that for $D_1 = 0.1$, $D_1 = 0.5$ and $D_1 = 1$ system is drawn towards the leukemic steady state as time goes to infinity. This can be seen in the corresponding simulations in Figure 4.3 where the dynamics approaches a fatal leukemic state. For the case with $D_1 = 5$ the figure shows that the dynamics are drawn to a stable co-existing state which is in accordance with the findings in Figure 4.3. This may be interpreted as the prognosis based on the model may change from a fatal leukemic state to a co-existing non-fatal state by increasing the T-cell specific immune response while fixing the other parameters. Thus the impact of including the T-cell response seems to be significant which is a motivating factor for considering the changes that occur by modifying the effect of this term.

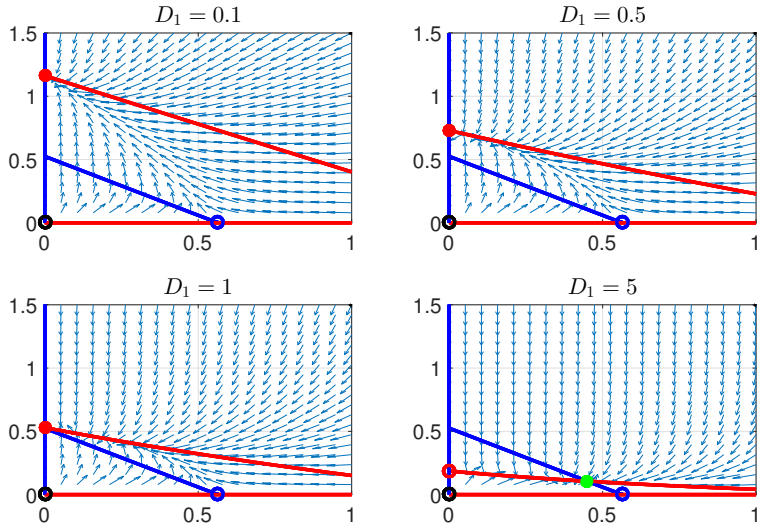

Figure 4.4: Phase portraits of the reduced T-cell model for increasing values of the parameter D_1 describing the strength of the T-cell specifik response. The black circle corresponds to a trivial fixed point, blue circles indicate hematopoietic fixed points, red circles corresponds to leukemic fixed points and green circles correspond to to co-existing fixed points. Full circles indicates that the fixed point is stable and open circles indicates an unstable fixed point.

4.4 The Modified T-cell Model

In the T-cell model in (4.12) it was assumed that $\eta \gg y_0$ meaning that the death rate of naive T-cells is significantly larger than the amount of malignant stem cells. As mentioned in the paper [34] the parameter for the death rate of naive T-cells η was estimated to $\eta \approx 0.04\,\mathrm{day}^{-1}$ indicating that this assumption might not be suitable based on the biology. Thus a new model is formulated where the T-cell response is based on (4.5) instead of (4.6). The modified y_0 dependent elimination term may be expressed

$$\gamma_{y_0} T_n \approx \gamma_{y_0} \frac{\alpha_n p_n}{\gamma_e} \frac{y_0}{y_0 + \eta} = \hat{d}_{y_0} \frac{1}{\eta + y_0} y_0.$$

Hence the model for the modified T-cell model is given by

$$\dot{x}_0 = (r_x \varphi_x(x_0, y_0) s - d_{x_0} - a_x) x_0, \tag{4.13a}$$

$$\dot{y}_0 = \left(r_y \varphi_y(x_0, y_0) s - d_{y_0} - \hat{d}_{y_0} \frac{1}{\eta + y_0} y_0 - a_y \right) y_0, \tag{4.13b}$$

$$\dot{x}_1 = a_x A_x x_0 - d_{x_1} x_1, \tag{4.13c}$$

$$\dot{y}_1 = a_y A_y y_0 - d_{y_1} y_1, \tag{4.13d}$$

$$\dot{a} = d_{x_0} x_0 + \left(d_{y_0} + \hat{d}_{y_0} \frac{1}{\eta + y_0} y_0 \right) y_0 + d_{x_1} x_1 + d_{y_1} y_1 - e_a s a, \tag{4.13e}$$

$$\dot{s} = r_s a - e_s s + I, \tag{4.13f}$$

where $\hat{d}_{y_0} = \gamma_{y_0} \frac{\alpha_n p_n}{\gamma_e}$. Note that $\hat{d}_{y_0}$ relates to $\tilde{d}_{y_0}$ from the T-cell model in (4.7) with the relation

$$\hat{d}_{y_0} = \gamma_{y_0} \frac{\alpha_n p_n}{\gamma_e \eta} \eta = \tilde{d}_{y_0} \eta.$$

From the relation it can be seen that the T-cell model relates to the modified T-cell model by providing an upper bound for the T-cell specific elimination given by

$$\hat{d}_{y_0} \frac{1}{\eta + y_0} y_0 \leq \hat{d}_{y_0} \frac{1}{\eta} y_0.$$

Let the functions g and h be defined by

$$g(y_0) = \hat{d}_{y_0} \frac{1}{\eta} y_0 \tag{4.14}$$

and

$$h(y_0) = \hat{d}_{y_0} \frac{1}{\eta + y_0} y_0, \tag{4.15}$$

where $\hat{d}_{y_0}$ and η are non-negative constants. The behavior of the functions g and h and their relation is further investigated in Figure 4.5 where the functions are depicted as a function of y_0 for different values of η. The figure shows that the approximation

$$h(y_0) \approx g(y_0), \tag{4.16}$$

is reasonable as long as $\eta \gg y_0$ but as y_0 increases and becomes equal to or larger than η, then $g(y_0)$ may not provide a good approximation for $h(y_0)$. From the function $h(y_0)$ it can be seen that the modified T-cell specific response term has a saturation since for a fixed value of η then $h(y_0) \to \hat{d}_{y_0}$ as $y_0 \to \infty$, i.e. the expression is approaching a constant and does not increase further with y_0 for y_0 large enough. Thus it is expected that the dynamics for $\eta \ll y_0$ will mimic the dynamics of the basic model in (4.1) where the y_0 elimination term is constant. The function $g(y_0) \to \infty$ as $y_0 \to \infty$ since the term keeps increasing linearly as a function of y_0 thus this function does not have a saturation for large values of y_0.

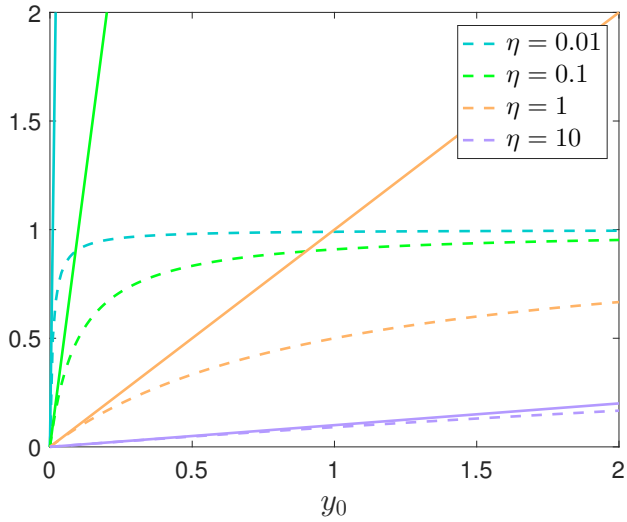

Figure 4.5: Plot of the functions $g(y_0)$ in (4.14) (full lines) and $f(y_0)$ in (4.15) (dashed lines) depicted as functions of y_0 for different values of η. The figure shows that the function g provides an upper bound for the function f. The figure also depicts how the quality of the approximation made in (4.16) is reasonable as long as $\eta \gg y_0$. Note that the plot is shown in dimensionless form and it is the ratio between y_0 and η which is the important factor. In the case that $\eta \ll y_0$ then the function f is approximately constant as y_0 increases further.

Thus comparing the T-cell model with the modified T-cell model it is expected

that the malignant stem cells are less restricted by the T-cell response in the modified T-cell compared to the T-cell model. It is therefore expected that the T-cell model will present a best case compared to the modified T-cell model and it may be possible that a parameter set which gives rise to a co-existing steady state for the T-cell model may give rise to dynamics approaching a leukemic steady state for the modified T-cell model.

4.4.1 Dimensionless Form

The modified T-cell model is brought into dimensionless form to reduce the number of parameters and number of equations. The scaling is chosen as for the T-cell model. Thus the dimensionless modified T-cell specific response may be expressed as

$$\begin{aligned}\frac{\hat{d}_{y_0}}{d_{x_0}+a_x}\frac{1}{\eta+\bar{y}_0 Y_0}\bar{y}_0 Y_0 \Leftrightarrow\\ \frac{\hat{d}_{y_0}}{d_{x_0}+a_x}\frac{1}{\frac{\eta}{\bar{y}_0}+Y_0}Y_0 \Leftrightarrow\\ \hat{D}_1\frac{1}{\kappa+Y_0}Y_0,\end{aligned}$$

where $\kappa = \frac{\eta}{\bar{y}_0}$ is the new introduced dimensionless parameter and $\hat{D}_1 = \frac{\hat{d}_{y_0}}{d_{x_0}+a_x}$ is independent of η. The constant $\hat{D}_1$ relates to the constant D_1 from the dimensionless T-cell model by

$$\hat{D}_1 = \frac{\hat{d}_{y_0}}{d_{x_0}+a_x} = \frac{\tilde{d}_{y_0}\eta\,\bar{y}_0}{(d_{x_0}+a_x)\bar{y}_0} = \frac{\tilde{d}_{y_0}\bar{y}_0}{d_{x_0}+a_x}\frac{\eta}{\bar{y}_0} = D_1\kappa.$$

Thus the relation between the modified T-cell model and the T-cell model is the same for the models in dimensionless form, i.e.

$$\hat{D}_1\frac{1}{\kappa+Y_0}Y_0 \leq \frac{\hat{D}_1}{\kappa}Y_0. \tag{4.17}$$

The relation in (4.17) implies that the approximation made in (4.10) also holds for the modified T-cell model. Hence the dimensionless T-cell modified model becomes

$$X_0' = \left(\frac{J+\sqrt{J^2+2B_xX_0+2B_yY_0}}{1+X_0+C_yY_0}-1\right)X_0, \tag{4.18a}$$

$$Y_0' = \left(R\frac{J+\sqrt{J^2+2B_xX_0+2B_yY_0}}{1+C_xX_0+Y_0}-D_0-\hat{D}_1\frac{1}{\kappa+Y_0}Y_0\right)Y_0. \tag{4.18b}$$

Note that $\kappa > 0$ and thus the right hand side of the model is still a C^1 function, i.e. we may apply the dynamical system theory presented in Chapter 3. Moreover there are not introduced new equations and only a single new parameter is added to the model. Thus this is a minor modification of the T-cell model and the complexity of the model is not increased dramatically by the modification.

In dimensionless form the amount of malignant stem cells does not exceed the value of 1 by much thus based on Figure 4.5 it is expected that for $\kappa \geq 10$ the modified T-cell model will be in accordance with the T-cell model and for $\kappa < 1$ it is expected that they are not in accordance.

4.4.2 Trapping Region

The existence of a trapping region is established to ensure the global existence and uniqueness of the modified T-cell model. The approach follows the approach for the T-cell model given in [1]. Consider the nonnegative orthant, i.e. the orthant obeying the biological restrictions that the amount of cells must be nonnegative. From the equations in (4.18) it follows that the y-axis is a nullcline for X_0 and that the x-axis is a nullcline for Y_0, this implies that if the solution for a given time t is in the nonnegative orthant then it must be in the nonnegative orthant for all time due to the existence and uniqueness of the initial value problem.

The idea is to establish a region by connecting the x-axis and y-axis with a line. This line should satisfy that $X_0' < 0$ and $Y_0' < 0$ on the line for large values of $X_0 + Y_0$ since this will ensure that the flow of the differential equation will point into the interior of the region or vanish. Consider the dimensionless reduced modified T-cell model in (4.18). Assuming that $X_0 > 0$ and $Y_0 > 0$ we would like to guaranty that the following relations are satisfied

$$\frac{J + \sqrt{J^2 + 2B_x X_0 + 2B_y Y_0}}{1 + X_0 + C_y Y0} - 1 < 0 \tag{4.19}$$

and

$$R\frac{J + \sqrt{J^2 + 2B_x X_0 + 2B_y Y_0}}{1 + C_x X_0 + Y0} - D_0 - \hat{D}_1 \frac{1}{\kappa + Y_0} Y_0 < 0. \tag{4.20}$$

Introducing

$$K = \max\left\{J, \sqrt{2B_x}, \sqrt{2B_y}\right\} \text{ and } L = \min\{1, C_x, C_y\}$$

Considering (4.19) and (4.20) then the following relations hold

$$\frac{J+\sqrt{J^2+2B_xX_0+2B_yY_0}}{1+X_0+C_yY_0}-1<\frac{K}{L}\frac{1+\sqrt{1+X_0+Y_0}}{1+X_0+Y_0}-1$$

and

$$\begin{aligned}
&R\frac{J+\sqrt{J^2+2B_xX_0+2B_yY_0}}{1+C_xX_0+Y0}-D_0-\hat{D}_1\frac{1}{\kappa+Y_0}Y_0\\
&<R\frac{K}{L}\frac{1+\sqrt{1+X_0+Y_0}}{1+X_0+Y_0}-D_0\\
&=D_0\left(\frac{R}{D_0}\frac{K}{L}\frac{1+\sqrt{1+X_0+Y_0}}{1+X_0+Y0}-1\right).
\end{aligned}$$

Note that since $D_0>0$ we need only to ensure that

$$\alpha\frac{1+\sqrt{1+X_0+Y_0}}{1+X_0+Y_0}-1<0,$$

where

$$\alpha=\frac{\max\left\{1,\frac{R}{D_0}\right\}\max\left\{J,\sqrt{2B_x},\sqrt{2B_y}\right\}}{\min\left\{1,C_x,C_y\right\}}.$$

Introducing

$$z=\sqrt{1+X_0+Y_0}, \tag{4.21}$$

reduces the problem to solve a 2. order polynomial, i.e.

$$z^2-\alpha z-\alpha>0.$$

Solving this polynomial yields the solution

$$z_{\text{sol}}=\frac{1}{2}\left(\alpha\pm\sqrt{\alpha^2+4\alpha}\right),$$

which has exactly one positive solution for all $\alpha>0$ since the square-root function is a monotonic increasing function for $\alpha>0$. From the definition of z we restrict that z_{sol} must in addition satisfy that $z_{\text{sol}}\geq 1$ since both X_0 and Y_0 are nonnegative, i.e. we may choose z as

$$z_{\text{sol}}=\max\left\{1,\frac{1}{2}\left(\alpha+\sqrt{\alpha^2+4\alpha}\right)\right\}.$$

Solving for X_0+Y_0 in (4.21) yields that the bound M is

$$M=z_{\text{sol}}^2-1.$$

Thus for $X_0+Y_0>M$ we have that $X_0'<0$ and $Y_0'<0$ and thereby the triangle defined by the x-axis, y-axis and the line $Y_0=M-X_0$ defines an trapping region for the reduced dimensionless modified T-cell model in (4.12).

4.4.3 Analysis by Descartes Rule of Sign

An analysis of the number of admissible fixed points is performed to investigate the dynamics of the equations. Thus this analysis may be used as a theoretical support for the later numerical simulations. We will consider trivial , hematopoietic, leukemic and co-existing steady states.

From the dimensionless modified T-cell model in (4.18) it can be seen that there exists a trivial steady state for all admissible choices of parameters.

A solution to the hematopoietic steady state is found as a solution to

$$\sqrt{J^2 + 2B_x X_0} = 1 + X_0 - J.$$

Assuming that $J < 1 + X_0$ the second order polynomial is obtained

$$X_0^2 - 2(J + B_x - 1)X_0 - (2J - 1) = 0. \tag{4.22}$$

The solution for this second order polynomial is

$$\begin{aligned} X_0 &= (J + B_x - 1) \pm \sqrt{(J + B_x - 1)^2 + (2J - 1)} \\ &= (J + B_x - 1) \pm \sqrt{(J + B_x)^2 - 2B_x}. \end{aligned}$$

The roots of the polynomial are real if and only if

$$J \geq -B_x + \sqrt{2B_x}.$$

However, note that the right hand side of the inequality satisfies that

$$-B_x + \sqrt{2B_x} \leq \frac{1}{2}, \quad \text{for all } B_x > 0.$$

Thus by choosing $J \geq \frac{1}{2}$ the roots are real for all choices of B_x. It can be seen from equation (4.22) that there for the choice of $J \geq \frac{1}{2}$ is exactly one change of sign in the coefficients of the polynomial and by applying Descartes Rule of sign [35] it can be concluded that for $\frac{1}{2} \leq J \leq 1$ there will be exactly one hematopoietic steady state. For the standard parameters shown in Table 4.3 it can be seen that the standard parameter choice for J satisfies that $\frac{1}{2} \leq J \leq 1$ thus for the simulations we can guarantee that there should be exactly one hematopoietic steady state.

A leukemic steady state is a solution of

$$R\frac{J + \sqrt{J^2 + 2B_x X_0 + 2B_y Y_0}}{1 + C_x X_0 + Y_0} - D_0 - \hat{D}_1 \frac{1}{\kappa + Y_0} Y_0 = 0,$$

which may be written as

$$(J^2 + 2B_y Y_0)(\kappa + Y_0)^2 = \left(\frac{D_0}{R}(1 + Y_0)(\kappa + Y_0) + \frac{\hat{D}_1}{R} Y_0(1 + Y_0) - J(\kappa + Y_0) \right)^2, \tag{4.23}$$

with the constraint that

$$\frac{D_0}{R}(1 + Y_0)(\kappa + Y_0) + \frac{\hat{D}_1}{R} Y_0(1 + Y_0) - J(\kappa + Y_0) \geq 0. \tag{4.24}$$

The expression in (4.23) can be rewritten into the standard form for 4. order polynomial

$$\alpha_1 Y_0^4 + \alpha_2 Y_0^3 + \alpha_3 Y_0^2 + \alpha_4 Y_0 + \alpha_5 = 0, \tag{4.25}$$

where $\alpha_1, \alpha_2, \alpha_3, \alpha_4$ and α_5 are constants depending on the parameters given by

$$\begin{aligned}
\alpha_1 &= \frac{D_0^2 + 2D_0\hat{D}_1 + \hat{D}_1^2}{R^2}, \\
\alpha_2 &= -\frac{(2D_0R + 2\hat{D}_1R)J}{R^2} + \frac{2D_0^2\kappa + 2D_0\hat{D}_1\kappa + 2D_0^2 + 4D_0\hat{D}_1 + 2\hat{D}_1^2}{R^2} - 2B_y, \\
\alpha_3 &= \frac{D_0^2\kappa^2 + 4D_0^2\kappa + 4D_0\hat{D}_1\kappa + D_0^2 + 2D_0\hat{D}_1 + \hat{D}_1^2}{R^2} \\
&\quad - \frac{(4\hat{D}_0R\kappa + 2\hat{D}_1R\kappa - 2D_0R - 2\hat{D}_1R)}{R^2} J - 4B_y\kappa, \\
\alpha_4 &= \frac{2D_0^2\kappa^2 + 2D_0^2\kappa + 2D_0\hat{D}_1\kappa}{R^2} - \frac{(2D_0R\kappa^2 - 4D_0R\kappa - 2\hat{D}_1R\kappa)}{R^2} J - 2B_y\kappa^2, \\
\alpha_5 &= \left(\frac{{D_0}^2}{R^2} - 2\,\frac{D_0\,J}{R} \right) \kappa^2.
\end{aligned}$$

From the expressions it can be seen that α_1 is positive for all admissible parameters and that if D_0 is chosen large enough then α_2, α_3,α_4 and α_5 will be positive since the second order D_0 terms will dominate the expressions. By Descartes rule of sign this means that there is no admissible leukemic steady state if D_0 is chosen large enough. However, if J is chosen large enough then α_2, α_3,α_4 are all negative and a leukemic steady state becomes inevitable. Thus the existence of a leukemic steady state depends on the same parameters as for the T-cell model which may be verified by comparing the found coefficients to those of the T-cell model presented in (A.1) in Appendix A.1.

The coefficients are expressed as a function of D_1 and κ with the standard parameters presented in Table 4.3 to examine if there is a leukemic steady state for the standard parameters and varying values of κ and D_1. The expressions

for the coefficients as a function of κ and D_1 based on the default parameters are

$$\begin{aligned}
\alpha_1 &= \hat{D}_1^2 + 2\hat{D}_1 + 1,\\
\alpha_2 &= (2\hat{D}_1^2 + 2\hat{D}_1\kappa + 1.7352\hat{D}_1 + 2\kappa - 0.575614),\\
\alpha_3 &= (\hat{D}_1^2 + 1.7352\hat{D}_1\kappa + \kappa^2 - 0.2648\hat{D}_1 - 1.151228\kappa - 1.264800),\\
\alpha_4 &= -(0.2648\hat{D}_1\kappa + 0.575614\kappa^2 + 2.529600\kappa),\\
\alpha_5 &= -1.264800000\kappa^2.
\end{aligned}$$

The expressions for the coefficients show that $\alpha_1 > 0$ and $\alpha_4, \alpha_5 < 0$ for all $\kappa, D_1 > 0$. Isolating κ in $\alpha_3 = 0$ yields a second order polynomial and isolating κ in $\alpha_2 = 0$ yields a linear function. The two functions are depicted as a function of D_1 in Figure A.1 in Appendix A.2. The figure shows that the sign of α_3 will change before α_2 for any choice of D_1 and κ. Both functions are continuous thus for any combination of D_1, $\kappa \geq 0$ there is exactly one sign change for the coefficients, i.e. by Descartes rule of sign there will be exactly one leukemic steady state for the standard parameters in 4.3 and any choice of $\kappa, D_1 > 0$ satisfying the constraint in (4.24).

A co-existing steady state is a solution of

$$J - \sqrt{J^2 + 2B_xX_0 + 2B_yY_0} = 1 + X_0 + C_yY_0 \tag{4.26}$$

and

$$J - \sqrt{J^2 + 2B_xX_0 + 2B_yY_0} = (1 + C_xX_0 + Y_0)\left(\frac{D_0}{R} + \frac{\hat{D}_1}{R}\frac{1}{\kappa + Y_0}Y_0\right). \tag{4.27}$$

If Y_0 is known then the expression for the co-existing X_0 can be found by subtracting (4.26) from (4.27) and isolating X_0. The expression for the co-existing X_0 as a function of the co-existing Y_0 becomes

$$X_0 = \frac{(1 + Y_0)\left(\frac{D_0}{R} + \frac{\hat{D}_1}{R}\frac{1}{\kappa+Y_0}Y_0\right) - C_yY_0 - 1}{1 - C_x\left(\frac{D_0}{R} + \frac{\hat{D}_1}{R}\frac{1}{\kappa+Y_0}Y_0\right)}.$$

Co-existing candidates for Y_0 are found as a solution to the 4. order polynomial obtained by substituting the expression for co-existing X_0 into (4.26), i.e.

$$\beta_1Y_0^4 + \beta_2Y_0^3 + \beta_3Y_0^2 + \beta_2Y_0 + \beta_1,$$

where the coefficient for this 4. order polynomial are shown in (A.2) Appendix A.3. Note that the solutions found must satisfy the constraints that

$$1 + X_0 + C_yY_0 > J \tag{4.28}$$

and

$$(1 + C_x X_0 + Y_0)\left(\frac{D_0}{R} + \frac{\hat{D}_1}{R}\frac{1}{\kappa + Y_0}Y_0\right) > J. \tag{4.29}$$

Note that the first constraint is trivially satisfied for the standard parameter choice of J. The expressions for the coefficients are not easily investigated analytically. Thus further analysis of the co-existing steady state is performed for specific parameter choices. The T-cell model reaches a co-existing steady state as depicted in Figure 4.4 in the case $D_1 = 5$. Thus to investigate how the modified T-cell model behaves as κ changes the two following cases are considered, namely the case where $\hat{D}_1 = 50$ and $\kappa = 10$ and the case where $\hat{D}_1 = 0.5$ and $\kappa = 0.1$. These two cases satisfy that $\frac{\hat{D}_1}{\kappa} = D_1 = 5$. In the first case with $\hat{D}_1 = 50$ and $\kappa = 10$ the following coefficients for the 4. order polynomial is obtained

$$\begin{aligned}
\beta_1 &= \ -0.98,\\
\beta_2 &= -16.57,\\
\beta_3 &= \ 242.53,\\
\beta_4 &= -18.21,\\
\beta_5 &= \ \ 0.02.
\end{aligned}$$

The coefficients change sign three times thus by Descartes rule of sign there will be 1 or 3 positive roots of the polynomial. The positive roots can be calculated explicit and they are given by

$$\begin{aligned}
Y_{0_1} &= \ \ 0.11,\\
Y_{0_2} &= \ 13.47,\\
Y_{0_3} &= 789.51.
\end{aligned}$$

It is found that only Y_{0_1} satisfies the constraints thus it is expected that there will be exactly one co-existing steady state and the dynamics of the modified T-cell model is expected to behave similar to the dynamics shown in Figure 4.4 for this specific choice of parameters.

In the second case with $\hat{D}_1 = 0.5$ and $\kappa = 0.1$ the following coefficients for the 4. order polynomial is obtained

$$\begin{aligned}
\beta_1 &= -0.98 \cdot 10^{-4},\\
\beta_2 &= -0.36 \cdot 10^{-2},\\
\beta_3 &= -0.17 \cdot 10^{-2},\\
\beta_4 &= -0.20 \cdot 10^{-3},\\
\beta_5 &= \ \ 1.96 \cdot 10^{-5}.
\end{aligned}$$

Thus by Descartes rule of sign there is exactly one positive real root. The root is found to be $Y_{0_1} = 16.35$. However, this root does not satisfy the constraints thus we cannot guarantee the existence of a co-existing steady state and it is expected that they may not be a co-existing steady state for this specific choice of parameters. Hence it is expected that the modified T-cell model may exhibit a different dynamics compared to the T-cell model for the same choices of parameters based on this analysis.

4.5 The Resistant T-cell Model

As mentioned in Chapter 2 biological theory, the effectiveness of the T-cell response may wear off with time due to the malignant cells becoming resistant to the T-cell response. A mathematical model for modeling the resistance is proposed in [1]. However, this model is based on a mathematical approach. The aim is to formulate a simple model desribing the phenomena based on biological assumptions instead. Thus the T-cell model will be extended to include resistant malignant stem cells inspired by the biological approach used in [36].

From a biological aspect, the malignant stem cells becoming resistant may be interpreted as the y_0 compartment being spilt into two compartments, namely a compartment with the malignant stem cells that have not acquired resistance to the T-cell response, z_0 and those who have acquired the resistance, z_r. Thus the total amount of malignant stem cells may be described by the sum of the two types of stem cells, i.e. $y_0 = z_0 + z_r$. At time t_0 we assume that the amount of resistant malignant stem cells are zero and as time evolve the malignant stem cells are allowed to turn into resistant stem cells. This approach is inspired by [36] where a model for CML including resistance of malignant cells i proposed. Assuming that the overall dynamics are similar to the T-cell model in (4.7), the dynamics of the malignant stem cells may be described by

$$\dot{z}_0 = \left(r_y \tilde{\varphi}_y(x_0, z_0, z_r)s - d_{y_0} - \tilde{d}_{y_0} z_0 - a_y\right) z_0 - \rho z_0, \tag{4.30a}$$

$$\dot{z}_r = \left(r_y \tilde{\varphi}_y(x_0, z_0, z_r)s - d_{y_0} - a_y\right) z_r + \rho z_0, \tag{4.30b}$$

where $\tilde{\varphi}_y(x_0, z_0, z_r) = \varphi_y(x_0, z_0 + z_r)$ and ρ is a function that depends on the resistance-biology and describes the how the non-resistant malignant stem cells turn resistant which will be referred to as the second mutation rate. Substituting the y_0 equation in the T-cell model with (4.30), yields the resistant T-cell model

$$\dot{x}_0 = (r_x\tilde{\varphi}_x(x_0, z_0, z_r)s - d_{x_0} - a_x)x_0, \tag{4.31a}$$
$$\dot{z}_0 = (r_y\tilde{\varphi}_y(x_0, z_0, z_r)s - d_{y_0} - \tilde{d}_{y_0}z_0 - a_y)z_0 - \rho z_0, \tag{4.31b}$$
$$\dot{z}_r = (r_y\tilde{\varphi}_y(x_0, y_0, z_r)s - d_{y_0} - a_y)z_r + \rho z_0, \tag{4.31c}$$
$$\dot{x}_1 = a_x A_x x_0 - d_{x_1}x_1, \tag{4.31d}$$
$$\dot{y}_1 = a_y A_y(z_0 + z_r) - d_{y_1}y_1, \tag{4.31e}$$
$$\dot{a} = d_{x_0}x_0 + (d_{y_0} + \tilde{d}_{y_0}z_0)z_0 + d_{y_0}z_r + d_{x_1}x_1 + d_{y_1}y_1 - e_a sa, \tag{4.31f}$$
$$\dot{s} = r_s a - e_s s + I, \tag{4.31g}$$

where $\tilde{d}_{y_0} = \gamma_{y_0}\frac{\alpha_n p_n}{\gamma_e \eta}$ describes the effect of the T-cell response in the same manner as in the T-cell model. Note that the sum of the two new equations satisfies that

$$\dot{y}_0 = \dot{z}_0 + \dot{z}_r = \left(r_y\tilde{\varphi}_y(x_0, z_0, z_r)s - a_y - d_{y_0} - \tilde{d}_{y_0}\frac{z_0^2}{z_0 + z_r}\right)(z_0 + z_r).$$

Hence as the malignant stem cells turn resistant, the effect of the T-cell response wears off and the equations mimics the behavior of the basic model without the T-cell response presented in (4.1) whereas as long as the resistant cells are negligible then the dynamics mimic the T-cell model in (4.7). Moreover, since the T-cell specific response is only included in the stem cell compartment we will not split the mature malignant cells into two compartments since these two compartments would be identical for this model formulation.

In the model proposed in [36] the function $\rho(z_0)$ was chosen as a constant. A model where $\rho(z_0)$ was a more complicated expression given by a hill function depending on the current exposure of malignant cells did not produce qualitative different results thus the simpler model is preferred by the parsimonious principle.

4.5.1 Dimensionless Form

The resistant T-cell model is brought into dimensionless form. For simplicity the same scaling constants are chosen as for the T-cell model. Thus the resistant

T-cell model in dimensionless form may be expressed by

$$X_0' = \left(\frac{J + \sqrt{J^2 + 2B_x X_0 + 2B_y(Z_0 + Z_r)}}{1 + X_0 + C_y(Z_0 + Z_r)} - 1 \right) X_0, \tag{4.32a}$$

$$Z_0' = \left(R\frac{J + \sqrt{J^2 + 2B_x X_0 + 2B_y(Z_0 + Z_r)}}{1 + C_x X_0 + (Z_0 + Z_r)} - D_0 - D_1 Z_0 - P \right) Z_0, \tag{4.32b}$$

$$Z_r' = \left(R\frac{J + \sqrt{J^2 + 2B_x X_0 + 2B_y(Z_0 + Z_r)}}{1 + C_x X_0 + (Z_0 + Z_r)} - D_0 \right) Z_r + PZ_0, \tag{4.32c}$$

where $R = \frac{r_y}{r_x}$, $C_x = \frac{c_{xy}}{c_{yy}}$, $C_y = \frac{c_{yx}}{c_{xx}}$, $D_0 = \frac{d_{y_0} + a_x}{d_{x_0} + a_x}$, $D_1 = \frac{\tilde{d}_{y_0}\bar{y}_0}{d_{x_0} + a_x}$ and $P = \frac{\rho}{d_{x_0} + a_x}$ describes the dimensionless second mutation rate.

4.5.2 Trapping Region

A trapping region can be established for the dimensionless resistant T-cell model in (4.32) to ensure that the solutions are well-behaved. Note that the Z_0-Z_r plane is a nullcline for X_0, i.e. X_0 cannot not cross this plane. Similarly the Z_0-Z_r plane is a nullcline for Z_0. If we have $X_0, Z_0 > 0$ at some time t then for all time $X_0, Z_0 \geq 0$. The Z_0 axis is a nullcline for Z_r but the Z_0-X_0 plane is not a nullcline for Z_r due to the PZ_0 term. However, since $Z_0 > 0$ and $Z_r' \to PZ_0 \geq 0$ as $Z_r \to 0$ thus the vector field will be positive with respect to Z_r for vanishing Z_0 and thus Z_r cannot become negative as long as Z_0 is nonnegative. Thus we may use the same argument for a trapping region as for the modified T-cell model, i.e. the aim is to show that for large choices of X_0, Z_0 and Z_r then $X_0' < 0$, $Z_0' < 0$ and $Z_r' < 0$.

First it is shown that for negative for large values of X_0, Z_0 and Z_r then $X_0' < 0$, $Z_0' < 0$ and $Z_0' + Z_r' < 0$ since if this holds then it follows that also $Z_r' < 0$. Consider the equations for X_0', Z_0' and $Z_0' + Z_r'$. Assuming that $X_0 > 0$, $Z_0 > 0$ and $Z_r > 0$ the aim is to show

$$\frac{J + \sqrt{J^2 + 2B_x X_0 + 2B_y(Z_0 + Z_r)}}{1 + X_0 + C_y(Z_0 + Z_r)} - 1 < 0, \tag{4.33}$$

$$R\frac{J + \sqrt{J^2 + 2B_x X_0 + 2B_y(Z_0 + Z_r)}}{1 + C_x X_0 + (Z_0 + Z_r)} - D_0 - D_1 Z_0 - PZ_0 < 0 \tag{4.34}$$

and

$$R\frac{J + \sqrt{J^2 + 2B_x X_0 + 2B_y(Z_0 + Z_r)}}{1 + C_x X_0 + (Z_0 + Z_r)} - D_0 - D_1\frac{Z_0^2}{(Z_0 + Z_r)} < 0. \tag{4.35}$$

This is equivalent to showing

$$\alpha \frac{1+\sqrt{1+X_0+Z_0+Z_r}}{1+X_0+Z_0+Z_r} - 1 < 0$$

with

$$\alpha = \frac{\max\left\{\frac{D_0}{R}, 1\right\} \max\left\{J, \sqrt{2B_x}, \sqrt{2B_y}\right\}}{\min\left\{1, C_x, C_y\right\}}.$$

Introducing

$$w = \sqrt{1+X_0+Z_0+Z_r}, \tag{4.36}$$

it reduces to show that we can choose w such that

$$\alpha w^2 - \alpha w - \alpha > 0.$$

This inequality is satisfied if w is chosen larger than

$$w_{\text{sol}} = \max\left\{1, \frac{1}{2}\left(\alpha + \sqrt{\alpha^2+4\alpha}\right)\right\}.$$

Solving for $X_0 + Z_0 + Z_r$ in (4.36) yields that the bound M is

$$M = w_{\text{sol}}^2 - 1.$$

Thus for $X_0 + Z_0 + Z_r > M$ it follows that $X_0' < 0$, $Z_0' < 0$ and $Z_r' < 0$ and thereby we may guarantee the existence of a trapping region for the resistant T-cell model.

Numerical Experiments with Simulations

In this chapter numerical experiments in form of simulations will be carried out for the three models, namely the T-cell model, the modified T-cell model and the resistant T-cell model. The numerical experiments will be based on the standard parameters given in Table 4.3 unless other is stated. The main focus of interest for the simulations regarding the modified T-cell model is to investigate the dynamics for varying strengths of the T-cell specific response, i.e. varying parameter values of $\hat{D}_1$ and κ. For the resistant T-cell the aim is to produce simulations which shows how the dynamics change with a resistant mutation.

5.1 Simulation Set-up

The initial conditions for the simulations will be based on the hematopoietic steady state in the basic model in (4.1) and the standard parameters given in Table 4.1. For a hematopoietic steady state we set y_0 and y_1 equal to zero. The remaining variables are then found to be

$$\begin{aligned} x_0 &= 1.00 \cdot 10^4, \\ x_1 &= 4.01 \cdot 10^{10}, \\ a &= 7.18 \cdot 10^2, \\ s &= 3.61. \end{aligned}$$

At time zero it is assumed that a malignant mutation of a stem cell has occurred and thus at $t = 0$ the malignant initial conditions are

$$\begin{aligned} y_0 &= 1, \\ y_1 &= 0. \end{aligned}$$

Furthermore, all the simulations will be presented in non-dimensionless form whereas the phase plan portraits will be depicted in dimensionless form. The simulations are made in MatLab and the code is provided in Appendix B.

5.2 The Modified T-cell Model

Two experiments will be carried out for the modified T-cell model. First its relation to the T-cell model will be investigated through simulations and phase plan portraits. Secondly, the effect of changing the parameter κ will be tested by simulations where all parameters except κ are kept fixed.

5.2.1 Comparing the Modified T-cell Model and the T-cell Model

To investigate how the modified T-cell model in (4.18) differs from the T-cell model we may consider numerical simulations of the modified T-cell model with the same parameters used for the simulation of the T-cell model in (4.12), i.e. the models will be compared for the same choices of parameters with the relation found in Chapter 4

$$D_1 = \frac{\hat{D}_1}{\kappa}. \tag{5.1}$$

Thus in the simulations where the modified T-cell model is compared to the T-cell model we will use this relation such that the all the parameters are the same and only change between the models is the T-cell specific elimination term, namely

$$\frac{\hat{D}_1}{\kappa + Y_0} Y_0 \quad \text{and} \quad \frac{\hat{D}_1}{\kappa} Y_0,$$

i.e. for the simulations where the two models are compared the value of D_1 is kept constant such that when varying κ the value of $\hat{D}_1$ will be adjusted such that the ratio in (5.1) is kept constant.

The numerical experiment is simulated for four different choices of κ, namely $\kappa = 0.01$, $\kappa = 0.1$, $\kappa = 1$ and $\kappa = 10$. The simulations are shown in Figure 5.1. In Figure 5.1 the full lines correspond to the healthy (blue) and malignant (red) stem cell amounts of the T-cell model with the standard parameters in Table 4.3. For the modified T-cell model both the healthy and malignant stem cells are depicted using the same color. The healthy stem cells are depicted with stipulated lines and the malignant stem cells are depicted with dotted lines. The figure shows that for large κ which based on Figure 5.1 seems to be $\kappa \geq 10$ the modified T-cell model is in accordance with the T-cell model. However, for small enough κ, the figure depicts that the models are not in accordance since for $\kappa \leq 0.1$ and $D_1 = 5$ the T-cell model approaches a co-existing steady

state whereas the modified T-cell model approaches a leukemic steady state. To illustrate this finding further Figure 5.2 depicts the scenario solely for $\kappa = 0.1$ and Figure 5.3 for solely for $\kappa = 10$.

The corresponding phase portraits are shown in Figure 5.4. For simplicity the figure only depicts the fixed points and the nullclines. The figure illustrates how the Y_0-nullcline changes as a function of κ, as the of κ decreases the leukemic steady state increases. Both figures indicate that for $\kappa \leq 0.1$ the co-existing steady state which the T-cell model approaches for $D_1 = 5$ is changed into a stable leukemic steady state for the modified T-cell model.

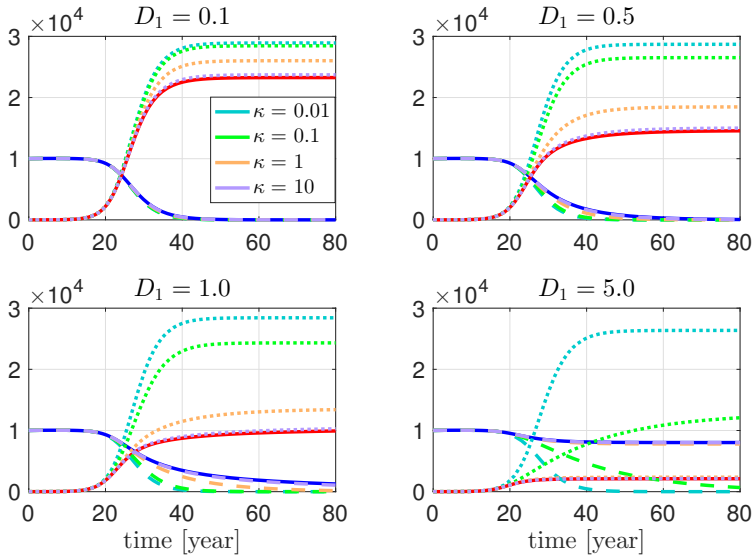

Figure 5.1: Simulation of reduced T-cell model in (4.12) (full lines) proposed in [1] and the modified T-cell model (4.18) for different values of the new model parameter κ. For the modified T-cell model both the healthy and malignant stem cells are depicted using the same color. The healthy stem cells are depicted with stipulated lines and the malignant stem cells are depicted with dotted lines. The simulations show that for small values of κ the simulations of the modified T-cell model are not in accordance with the T-cell model whereas for larger values of κ the modfied T-cell is in accordance with the T-cell model.

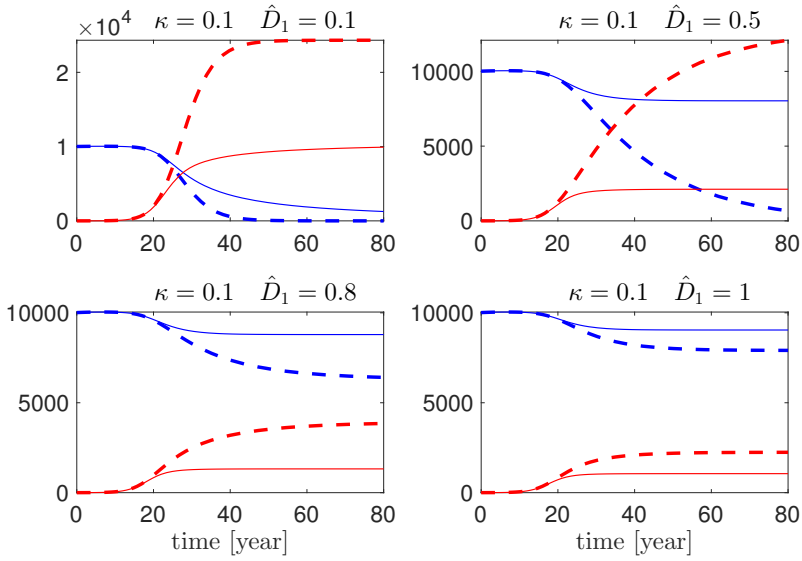

Figure 5.2: Simulations comparing the modified T-cell model (stippled lines) with standard parameters in Table 4.3 with varying values of $\hat{D}_1$ and $\kappa = 0.1$ to the T-cell model (full lines) for the same choice of parameters and the relation $\hat{D}_1 = D_1\kappa$. For this choice of κ the modified T-cell model is not in accordance with the T-cell model.

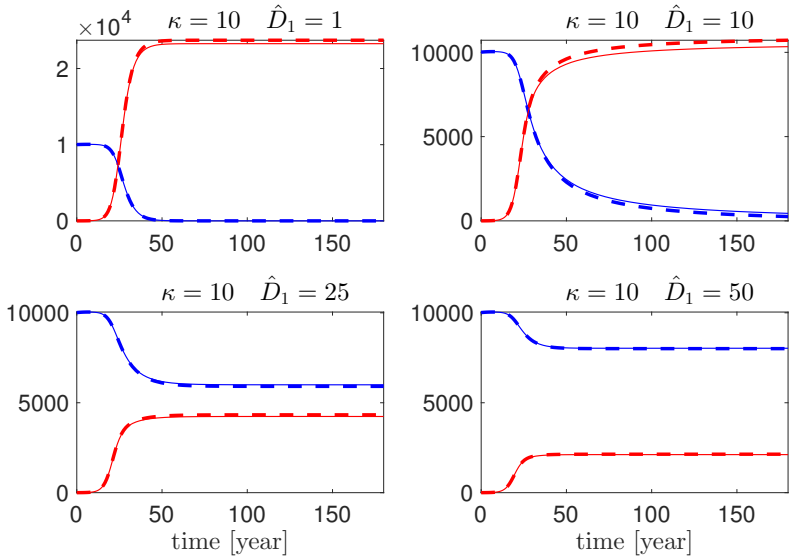

Figure 5.3: Simulations comparing the modified T-cell model (stippled lines) with standard parameters in Table 4.3 with varying values of $\hat{D}_1$ and $\kappa = 10$ to the T-cell model (full lines) for the same choice of parameters and the relation $\hat{D}_1 = D_1\kappa$. For this choice of κ the modified T-cell model is in accordance with the T-cell model.

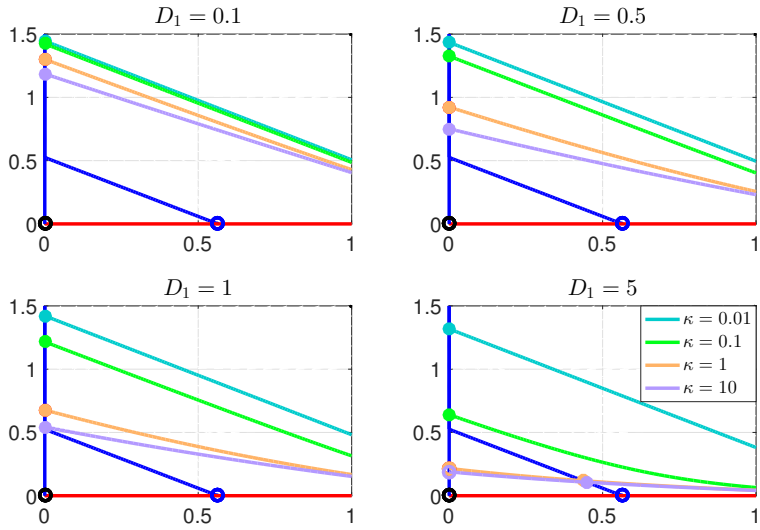

Figure 5.4: Nullcines and fixed points for the modified T-cell model in (4.18) with $\kappa = 0.1, 0.5, 1, 10$. The Y_0-nullcline is coloured such that it can be matched with the corresponding κ value. Moreover, the nullclines that do not change depending on κ are red if they are Y_0 nullclines and blue if they are X_0 nullclines. For $D_1 = 5$ the phase portrait changes from a phase portrait with a stable co-existing fixed point to a stable leukemic fixed point. The phaseportraits show that for large values of κ the phase plan portrait is similar to the phase plan portrait for the T-cell model depicted in Figure 4.4.

The phase portraits are shown for larger values of D_1 in Figure 5.5. Figure 5.5 shows that for some D_1 value between $D_1 = 6$ and $D_1 = 7$ the dynamics of the modified T-cell model shift from approaching a leukemic steady state to a co-existing steady state for the choice $\kappa = 0.1$. The figure also indicates that in the case that for large values of D_1 then $\kappa = 1$ and $\kappa = 10$ is approximately the same. However, for a value of $\kappa = 0.01$ the dynamics of the modified t-cell model does not shift from a leukemic steady state to a co-existing steady state indicating that a much larger increase in D_1 is need to change the dynamics of the modified T-cell model from a leukemic steady state to a co-existing steady state for small values of κ. Another finding is that for large values of κ the figure shows that even though the value of D_1 is doubled the co-existing steady state barely moves indicating that it may not be possible or require an unrealistic value of D_1 to change the dynamics from approaching a co-existing steady state into approaching a hematopoietic steady state. Thus the T-cell response may only hold the malignant cells down but not eradicate them since this would require an unrealistic large value for D_1 for the standard parameters.

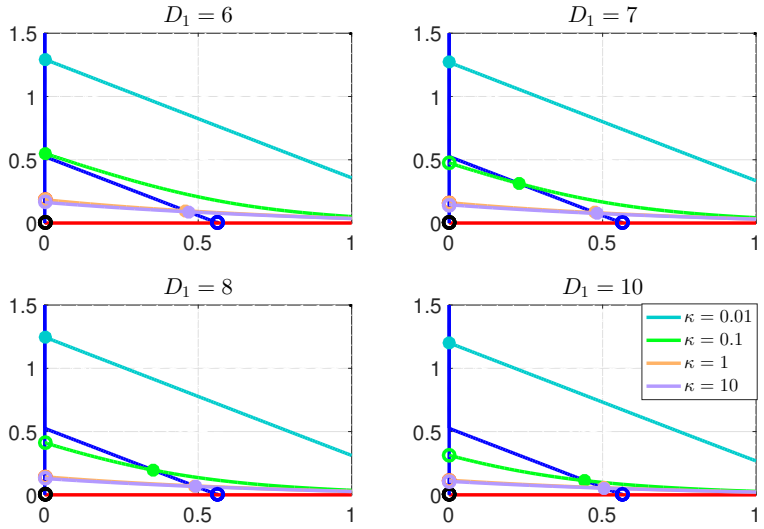

Figure 5.5: Nullcines and fixed points for the modified T-cell model in (4.18) with $\kappa = 0.01, 0.1, 1, 10$ and values of $D_1 = 6, 7, 8, 10$ where $D_1 = \frac{\hat{D}_1}{\kappa}$. The Y_0-nullcline is coloured such that it can be matched with the corresponding κ value. Moreover, the nullclines that do not change depending on κ are red if they are Y_0 nullclines and blue if they are X_0 nullclines.

5.2.2 The Effect of Changing the Death Rate of Naive T-cells

Simulations of the modified T-cell model are made for varying values of $\hat{D}_1$ and κ to investigate the effect of changing the parameter κ. These simulations are shown in Figure 5.6. The figure shows that as κ increases so does the amount of the malignant stem cells. For the parameter value $\hat{D}_1 = 1$ the simulations show that for $\kappa = 0.1$ and $\kappa = 0.001$ the dynamics of the model approach a co-existing steady state and for $\kappa = 1$ and $\kappa = 10$ the dynamics of the model approach a leukemic steady state. This behavior of the model is further supported by the corresponding phase plan portrait shown in Figure 5.7. Thus the simulations indicates that a small value of κ is preferable.

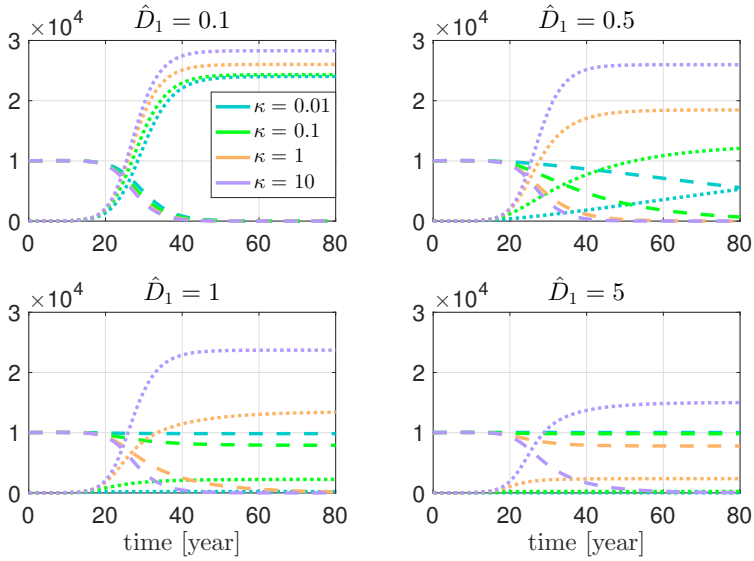

Figure 5.6: Simulations of the modified T-cell model with standard parameters in Table 4.3 with varying values of $\hat{D}_1$ and κ. The stipulated lines corresponds to the amount of healthy stem cell and the dotted lines indicate the amount of malignant stem cells. The figure shows that the maximal amount of malignant stem cells increases for increasing values of κ.

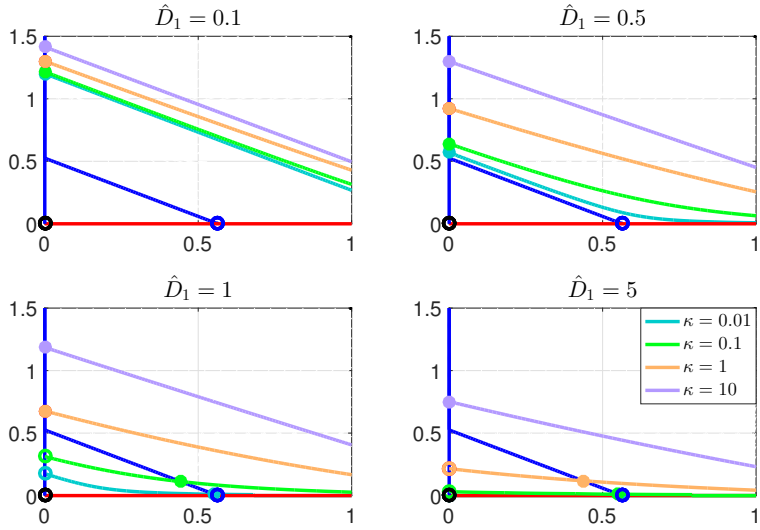

Figure 5.7: Nullcines and fixed points for the modified T-cell model in (4.18) with $\kappa = 0.01, 0.1, 1, 10$ and values of $\hat{D}_1 = 0.1$, 0.5, 1, 5. The Y_0-nullcline is coloured such that it can be matched with the corresponding κ value. Moreover, the nullclines that do not change depending on κ are red if they are Y_0 nullclines and blue if they are X_0 nullclines.The figure shows that small values of κ is preferable.

5.3 The Resistant T-cell Model

Simulations are carried out for the resistant T-cell model in (4.31) using the dimensionless form in (4.12) and the standard parameters in Table 4.3. Simulations of the resistant T-cell model and the T-cell model are depicted in Figure 5.8 with the dimensionless second mutation rate chosen as $P = 10^{-4}$ corresponding to the second mutation rate $\rho = 2 \cdot 10^{-7}$. The T-cell model is depicted with full lines where the blue line corresponds to the amount of healthy stem cells and the red line corresponds to the amount of malignant stem cells. The stipulated lines depict the resistant T-cell model where blue is the amount of healthy stem cells, red are the total amount of malignant stem cells, orange is the amount of resistant malignant stem cells and green is the amount of the non-resistant stem cells. The figure shows that in the case where the T-cell response successfully manage to keep the malignant stem cells at a co-existing state then as the malignant cells turn resistant, this co-existing state is lost and a fatal growth begins.

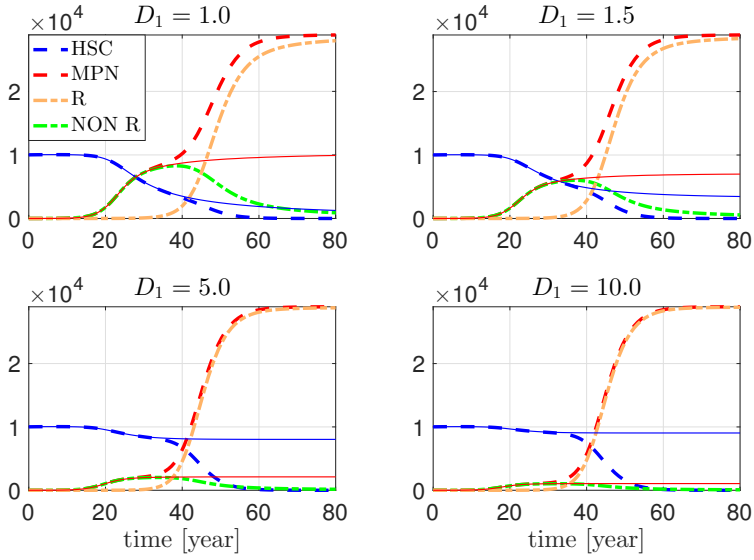

Figure 5.8: Simulations of the resistant T-cell model and the T-cell model with the standard parameters and $P = 10^{-4}$. The full lines corresponds to the T-cell model. The stipulated lines correspond to the resistant T-cell model where blue is the amount of healthy stem cells (HSC), red are the totalt amount of malignant stem cells (MPN), orange is the amount of resistant malignant stem cells (R) and green is the amount of the non-resistant stem cells (NON-R).

Discussion

The T-cell model presented in [1] is based on the parsimonious principle and all interactions are chosen to be first or second order. In the model it is assumed that the death rate of naive T-cells η is significantly larger than the amount of malignant stem cells, i.e. $\eta \gg y_0$. This assumption results in the following approximation

$$\frac{\hat{d}_{y_0}}{\eta + y_0} y_0 \approx \frac{\hat{d}_{y_0}}{\eta} y_0 = \tilde{d}_{y_0} y_0.$$

Thus this assumption is a simplifying assumption resulting in a linearization of a nonlinear Michaelis Menten term. In [34] an estimate for the death rate of naive T-cells is found to be $\eta \approx 0.04\,\mathrm{day}^{-1}$. This indicates that the assumption may not be appropriate and this is further supported by Figure 4.5 where the nonlinear Michaelis-Menten term is depicted with the corresponding linearization. Thus we formulate a new model where the assumption that $\eta \gg y_0$ is not used and this model is referred to as the modified T-cell model. The modified T-cell model is presented in (4.13). The model is brought into dimensionless form in (4.18) to reduce the number of parameters and a quasi steady state approximation is applied to reduce the number of equations. The dimensionless modified T-cell model is reduced to two equations and the further analysis of the death rate of naive T-cell cells will be discussed in terms of the dimensionless model and the dimensionless death rate of naive T-cell cells denoted by κ. A small value of κ is referring to $\kappa < 1$ since the amount of malignant stem cells are expected to be in the range $0 \leq Y_0 \leq 1.5$, whereas a large value of κ is expected to be $\kappa > 1$. Note that $\eta \approx 0.04$ corresponds to $\kappa \approx 2 \cdot 10^{-6}$ thus this value is considered a small value of κ.

For the modified T-cell model it was possible to establish an trapping region for any admissible choice of parameters and thereby ensure that the solutions of the model are well behaved. Moreover, it was shown that exactly one hematopoietic fixed point and one leukemic fixed point existed for the standard parameters by Descartes rule of sign. The analysis further showed that existence of a co-existing fixed point depends on several parameters. In the case where all parameters and the ratio κ and $\hat{D}_1$ were fixed, the analysis showed that these parameters may change if a co-existing fixed point was guaranteed to exists or not. In particular it was shown that the existence of an co-existing fixed point could be guaranteed for the choice $\kappa = 10$ and $\hat{D}_1 = 50$ whereas there could not be guaranteed the existence of an co-existing fixed point for $\kappa = 0.1$ and $\hat{D}_1 = 0.5$. These two cases was of particular interest due to the fact that they may both be compared to the simulation of the T-cell model with the parameter $D_1 = 5$. For this set of parameters the Figure 4.4 showed a co-existing fixed point for the T-cell model in [1]. Thus this analysis showed that the T-cell model is a best case

scenario compared to the modified T-cell model. The relation in (4.17) between the modified T-cell model and the T-cell model indicated that the T-cell model would be in accordance with the modified T-cell model for large values of κ whereas for small values of κ they might not be in accordance.

The relation between the modified T-cell model and the T-cell model was investigated in the numerical experiment in subsection 5.2.1. The numerical experiment is depicted in Figure 5.1, Figure 5.2 and Figure 5.3. The figures show that for $\kappa = 10$ and $\hat{D}_1 = 50$ the solution approaches a co-existing steady state whereas for $\kappa = 0.1$ and $\hat{D}_1 = 0.5$ the solution approaches a leukemic steady state which is consistent with the analytic findings. Namely, that the T-cell model with $D_1 = \frac{\hat{D}_1}{\kappa}$ does provide a best case scenario for the same set of parameters and that the difference between the T-cell model and the modified T-cell model increases as κ decreases.

The phase portrait in Figure 5.4 shows that as D_1 increases (corresponding to an increase in $\hat{D}_1$) , the value of the leukemic fixed point decreases. Especially for $\kappa = 0.1$ indicating that an even larger increase in D_1 might result in the emerge of a co-existing fixed point. Thus in Figure 5.5 the numerical experiment is repeated but for higher values of D_1. The figure shows that for a value some value $6 \leq D_1 \leq 7$ the stable leukemic fixed point turns unstable and a stable co-existing fixed point emerges. However, for the choice $\kappa = 0.01$ the figure shows that the leukemic fixed point is barely decreased thus for very small values of κ, a much larger and maybe even an unrealistic increase in D_1 is needed to change the stable leukemic fixed point into an unstable fixed point. Thus this contributes further to the analysis that showed that the difference in the two model increases as κ decreases. Interpreted in terms of clinical meaning, it indicates that if the parameters were estimated for a specific patient then it is possible that the T-cell model would indicate that a certain amount of treatment for example with T-cell therapy would be sufficient to avoid a fatal prognosis whereas the same treatment would not be sufficient for the patient in the modified T-cell model.

However, this analysis is solely based on comparing the two models and the effect of changing the parameter κ was investigated in the numerical experiment in subsection 5.2.2. The simulations in Figure 5.6 showed that a low value of κ is preferable for the outcome of the model since the figure shows that the maximal malignant stem cell amount for all time is decreased as κ decreases. κ describes the dimensionless death rate of naive T-cells thus this may be interpreted as a patient with a small death rate of naive T-cell have a larger amount of naive T-cell whereby the effector T-cell response is increased and thereby provide a better response to the malignant cells.

The possibility of the malignant cells becoming resistant to therapy is a known problem within gene- and immune therapy. Thus this was a motivating factor for formulating a model including resistance. The resistant model is based on the T-cell model in [1] with the addition of a new line of malignant stem cells that does not respond to the T-cell specific response. The resistant model is formulated in (4.31) where the parameter ρ describes the second mutation rate. Like for the modified T-cell model the model was brought into dimensionless form. The inclusion of the resistant malignant stem cell line resulted in a system of three equations instead of two which complicated the analysis. However, by similar considerations as for the modified T-cell model it was possible to establish a trapping region for all admissible choices of parameters. At first, a more complicated model for modeling resistance was formulated but the simulations did not show any qualitative difference in the simulations. Thus in this process of formulating the model has been an iterative process as illustrated by the moeling cycle in Figure 4.1 since at first the complicated model was proposed due to the belief that a simple model with ρ as a constant would not be able to capture the dynamics which was expected by the current perception of the resistance phenomena. However, by inspiration from [36] a simpler model was formulated and this simpler model was preferred by the parsimonious principle.

In section 5.3 a numerical experiment was performed to investigate the dynamics of the resistant T-cell model. The simulations are shown in Figure 5.8. The figure illustrates that at first the non-resistant malignant cells grow in numbers but after a time of exposure they turn resistant resulting in a growth of the resistant malignant cells and a decrease in the non-resistant malignant cells. This can be seen in all four simulations by considering the green stipulated line describing the amount of non-resistant malignant cells and the orange stipulated line describing the amount of resistant malignant cells. For the simulations with $D_1 = 5$ and $D_1 = 10$ a co-existing steady state is reached as for the T-cell model, but after some time of exposure the non-resistant malignant cells turn resistant and the growth of the non-resistant malignant stem cells eventually suppress both the healthy stem cells and the non-resistant line of malignant stem cells. Thus the simulations shows that resistance may result in that the co-existing steady state is lost and a fate growth begins. Thus this may be interpreted as patients receiving T-cell therapy and then the malignant stem cells turn immune despite continuous treatment. Another interpretation could be that patients may develop cancer even though they have an apparently normal immune system due to resistance. Thus the findings in the numerical experiment aligns with the expected theory of resistance described in the biological theory chapter.

The numerical experiment in Figure 5.8 for the resistant T-cell model showed behavior similar to the more mathematical based resistant model proposed in [1]. The models may be compared based on their complexity and their biological interpretation. In their dimensionless form they both have 3 differential

equations and variables. In the mathematical resistant model the third variable is a non-biological variable U describing the exposure after some time thus the new equation is $U' = Y_0$. The variable U is then introduced into the equation for Y_0 by a Hill function, i.e.

$$H(U) = \frac{1}{U^{\alpha} + 1},$$

where the biological interpretation of the parameter α is somewhat more complicated than the interpretation of the parameter introduced by the resistant T-cell model in this project. Thus the resistant model presented in this project may be preferred due to the parsimonious principle and the fact that the model is solely based on a biological perception of the resistance theory.

As mentioned all of the models have been brought into dimensionless form. The advantages of this approach are clearly seen by the reduction in number of parameters and the reduced number of equations. Moreover, the new parameters in these models are ratios indicating that the important parameters for the dynamics of the model may be the ratio and not the single parameter. An example of this is the parameter denoted by R describing the self-renewal ratio between the two self-renewal rates rather than the self-renewal rate of the malignant cells. Thus the analysis of the dimensionless form reveals some important dynamics of the system. However, in the T-cell model the number of parameters is 8 which may still be considered as a rather large amount of parameters. Thus further insight may be granted by analyzing the parameters by applying sensitivity analysis. This analysis might help determine which parameters are sensitive and which might not be as sensitive. Thus the less sensitive parameters may be considered less prone to change the outcome of the model and interpreted in terms of clinical validation these parameters may not need to be estimated for the individual patient. This might be a great advantage due to the possible challenges regarding collecting useful data for the model. The data collected by the doctors are mostly based on patients that currently receive treatment. Thus the parameters may already be affected by the treatment and thus suitable data may be hard to come by. Moreover, some of the parameters may be hard to estimate whereby a validation of the model is further complicated.

Conclusion

The T-cell model proposed in [1] for modeling the development of MPN shows that inflammation may trigger and drive blood cancer and that by boosting the body's own defence against foreign invaders the prognosis for a patient may be improved. In the model they have chosen an approximation based on the assumption that the death rate of naive T-cells is much larger than the amount of malignant cells. However, the estimate of this death rate is proposed to be approximately 0.004 in [34] indicating that it might not be a suitable assumption. The modified T-cell model where this assumption is avoided showed behavior similar to the T-cell model. However, the values of parameters for which a co-existing steady state was obtained with the T-cell model was turned into a leukemic steady state for the modified T-cell model. Analysis of the modified T-cell showed that the solutions of the model are well behaved and thus the modified T-cell model possesses desirable qualities for modeling biological systems.

Secondly, an attempt of formulating a model describing that the malignant cells may turn resistant to the T-cell response was successful. Analysis of the resistant T-cell model showed that the solutions of the model are well behaved which indicates that the model might be suitable to model the resistance phenomena for MPN. The simulations of the resistant T-cell model may be interpreted as when resistance occurs a successful T-cell therapy where the patient might live with a low amount of malignant cells might turn into a fatal scenario despite continued T-cell therapy. The model may also describe the scenario where a healthy person develop MPN despite having a normal immune response. Thus the mathematical models may be used to obtain a new insight for doctors and researchers within the area of cancerous diseases and may be used as guideline for which type of treatment might be preferable. Thus the potential for further research with mathematical models may have even greater influence in the future as awareness of mathematical modeling increases.

Bibliography

[1] M. Andersen, Z. Sajid, R. K. Pedersen, J. Gudmand-Hoeyer, C. Ellervik, V. Skov, L. Kjær, N. Pallisgaard, H. C. Hasselbalch, and J. T. Ottesen. Coupling blood cancers and inflammation: the reduced Cancitis model [Not published yet].

[2] Peter J. Campbell and Anthony R. Green. The myeloproliferative disorders. *New England Journal of Medicine*, 355(23):2452–2466, 2006. PMID: 17151367.

[3] Alfio Quarteroni. Mathematical models in science and engineering. 2008.

[4] M. Andersen, Z. Sajid, R. K. Pedersen, J. Gudmand-Hoeyer, C. Ellervik, V. Skov, L. Kjær, N. Pallisgaard, T. A. Kruse, M. Thomassen, J. Troelsen, H. C. Hasselbalch, and J. T. Ottesen. Mathematical modelling as a proof of concept for MPNs as a human inflammation model for cancer development. *PLoS ONE*, August 2017.

[5] David W Brown, Wayne H Giles, and Janet B Croft. White blood cell count. *Journal of Clinical Epidemiology*, 54(3):316–322, 2018/04/13.

[6] Vagn Juhl Larsen, Kirsten Selchau, and Henning Troelsen. *Gyldendals Minilex Biologi*. Gydendal, 2001.

[7] Eric M. Pietras, Matthew R. Warr, and Emmanuelle Passegué. Cell cycle regulation in hematopoietic stem cells. *The Journal of Cell Biology*, 195(5):709–720, 2011.

[8] L. A. Anderson and M. F. McMullin. Epidemiology of mpn: What do we know? *Current Hematologic Malignancy Reports*, 9(4):340–349, Dec 2014.

[9] David Dingli and Franziska Michor. Successful therapy must eradicate cancer stem cells. *STEM CELLS*, 24(12):2603–2610, 2006.

[10] Geoffrey M Cooper. *The Cell: A Molecular Approach. 2nd edition*. Sinauer Associates, 2000.

[11] Iñigo Martincorena and Peter J. Campbell. Somatic mutation in cancer and normal cells. *Science*, 349(6255):1483–1489, 2015.

[12] D. S. Alberts and L. M. Hess. Introduction to cancer prevention. *Fundamentals of Cancer Prevention*, pages 1–12, 2005.

[13] Glen J. Titmarsh, Andrew S. Duncombe, Mary Frances McMullin, Michael O'Rorke, Ruben Mesa, Frank Vocht, Sarah Horan, Lin Fritschi, Mike

Clarke, and Lesley A. Anderson. How common are myeloproliferative neoplasms? a systematic review and meta-analysis. *American Journal of Hematology*, 89(6):581–587.

[14] Manash K Paul and Anup K Mukhopadhyay. Tyrosine kinase –role and significance in cancer. *International Journal of Medical Sciences*, 1(2):101–115, 2004.

[15] L.G De Pillis and A Radunskaya. The dynamics of an optimally controlled tumor model: A case study. *Mathematical and Computer Modelling*, 37(11):1221 – 1244, 2003. Modeling and Simulation of Tumor Development, Treatment, and Control.

[16] Eda Tanrikulu Simsek, Ahmet Emre Eskazan, Mahir Cengiz, Muhlis Cem Ar, Seda Ekizoglu, Ayse Salihoglu, Emine Gulturk, Tugrul Elverdi, Seniz Ongoren Aydin, Ahu Senem Demiroz, Ayse Nur Buyru, Zafer Baslar, Ugur Ozbek, Burhan Ferhanoglu, Yildiz Aydin, Nukhet Tuzuner, and Teoman Soysal. Imatinib reduces bone marrow fibrosis and overwhelms the adverse prognostic impact of reticulin formation in patients with chronic myeloid leukaemia. *Journal of Clinical Pathology*, 69(9):810–816, 2016.

[17] Thomas O'Hare, Christopher A Eide, and Michael W Deininger. New bcr-abl inhibitors in chronic myeloid leukemia: keeping resistance in check. *Expert Opinion on Investigational Drugs*, 17(6):865–878, 2008. PMID: 18491988.

[18] Rosane Isabel Bittencourt, Jose Vassallo, Maria de Lourdes Lopes Ferrari Chauffaille, Sandra Guerra Xavier, Katia Borgia Pagnano, Ana Clara Kneese Nascimento, Carmino Antonio De Souza, and Carlos Sergio Chiattone. Philadelphia-negative chronic myeloproliferative neoplasms. *Revista Brasileira de Hematologia e Hemoterapia*, 34(2):140–149, 2012.

[19] Magnus Bjorkholm, AAsa R. Derolf, Malin Hultcrantz, Sigurdur Y. Kristinsson, Charlotta Ekstrand, Lynn R. Goldin, Bjorn Andreasson, Gunnar Birgegaard, Olle Linder, Claes Malm, Berit Markeværn, Lars Nilsson, Jan Samuelsson, Fredrik Granath, and Ola Landgren. Treatment-related risk factors for transformation to acute myeloid leukemia and myelodysplastic syndromes in myeloproliferative neoplasms. *Journal of Clinical Oncology*, 29(17):2410–2415, 2011. PMID: 21537037.

[20] Lisa M Coussens and Zena Werb. Inflammation and cancer. *Nature*, 420(6917):860–867, 12 2002.

[21] Sergei I. Grivennikov, Florian R. Greten, and Michael Karin. Immunity, inflammation, and cancer. *Cell*, 140(6):883–899, 2018/03/19.

[22] Domenico Ribatti. The concept of immune surveillance against tumors: The first theories. *Oncotarget*, 8(4):7175–7180, 01 2017.

[23] Scott McComb, Aude Thiriot, Lakshmi Krishnan, and Felicity Stark. *Introduction to the Immune System*, pages 1–20. Humana Press, Totowa, NJ, 2013.

[24] Alan Aderem. Phagocytosis and the inflammatory response. *The Journal of Infectious Diseases*, 187(Supplement 2):S340–5, 2003.

[25] Martin S.Blumenreich. The white blood cell and differential count.

[26] AI Lamond. Molecular biology of the cell, 4th edition. *Nature*, 417(6887):383–383, 2002.

[27] Peter S. Kim, Peter P. Lee, and Doron Levy. Modeling regulation mechanisms in the immune system. *Journal of Theoretical Biology*, 246(1):33 – 69, 2007.

[28] Lawrence Perko. Differential equations and dynamical systems. *Siam Review*, 34(1):129–131, 1992.

[29] C. Robinson. *Dynamical systems. Stability, symbolic dynamics, and chaos.* CRC Press„ 1995.

[30] *Ordinary Differential Equations with Applications.* Springer New York, 2006.

[31] An introduction to mathematical modelling glenn marion, bioinformatics and statistics scotland, 2008.

[32] T. H. Kjeldsen M. Blomhoej and J. T. Ottesen. Compartment models. 2018.

[33] Sumeet Agarwal, Kevin Burrage, and Simon Davis. Mathematical modeling of t-cell receptor triggering and activation. 2008.

[34] Hiroshi Mohri, Alan S Perelson, Keith Tung, Ruy M Ribeiro, Bharat Ramratnam, Martin Markowitz, Rhonda Kost, Hurley, Leor Weinberger, Denise Cesar, Marc K Hellerstein, and David D Ho. Increased turnover of t lymphocytes in hiv-1 infection and its reduction by antiretroviral therapy. *The Journal of Experimental Medicine*, 194(9):1277–1288, 11 2001.

[35] Xiaoshen Wang. A simple proof of descartes's rule of signs. 111, 06 2004.

[36] Franziska Michor, Timothy P. Hughes, Yoh Iwasa, Susan Branford, Neil P. Shah, Charles L. Sawyers, and Martin A. Nowak. Dynamics of chronic myeloid leukaemia. *Nature*, 435:1267 EP –, 06 2005.

Appendix

A.1 Leukemic Coefficients for the T-cell Model

$$\alpha_1 = \frac{{D_1}^2}{R} \tag{A.1a}$$

$$\alpha_2 = 2\frac{D_1}{R}\left(\frac{D_1}{R} + \frac{D_0}{R}\right) \tag{A.1b}$$

$$\alpha_3 = \left(\frac{D_0}{R}\right)^2 + \left(\frac{D_1}{R}\right)^2 + 2\frac{D_1}{R}\left(\frac{D_0}{R} - J\right) \tag{A.1c}$$

$$\alpha_4 = 2\left(\left(\frac{D_0}{R} - J\right)\left(\frac{D_0}{R} + \frac{D_1}{R}\right) - B_y\right) \tag{A.1d}$$

$$\alpha_5 = \frac{D_0}{R)}\left(\frac{D_0}{R} - 2J\right) \tag{A.1e}$$

A.2 Sign Change for Leukemic Coefficients

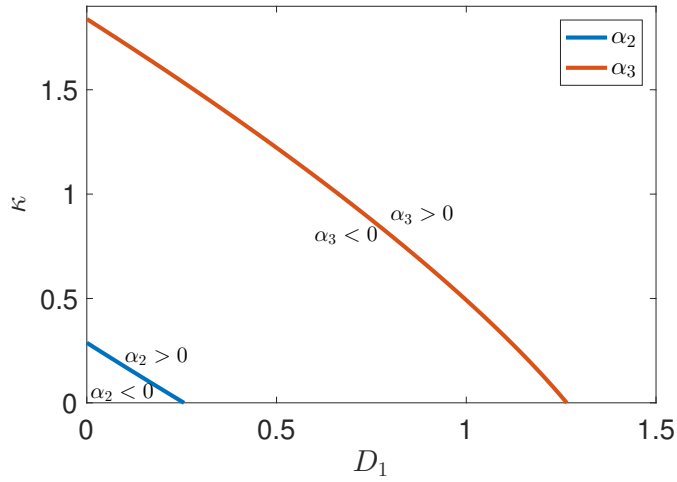

Figure A.1: The figure shows the line for which the coefficients α_2 and α_3 change sign in the polynomial describning the leukemic steady state in (4.25). For both coefficients it holds that they are positive for sufficiently large values of κ and $\hat{D}_1$. It can be seen that the coefficient α_3 changes sign before α_2 for all choices of $\hat{D}_1$.

A.3 Co-Existence Coefficients for the Modified T-cell Model

$$\beta_1 = -\left(D_0 + \hat{D}_1\right)^2 (C_x C_y - 1)^2 \tag{A.2a}$$

$$\begin{aligned}\beta_2 = {} & 2\,((-\kappa {C_y}^2 + (J-1)C_y + B_y)D_0 \\ & + \hat{D}_1\,((J-1)C_y + B_y))(D_0 + \hat{D}_1){C_x}^2 \\ & - 2\,(((-2\,\kappa - 1)C_y + J + B_x - 1)D_0 + (J + B_x - C_y - 1)\hat{D}_1 \\ & + ((J - B_x)C_y + 2\,B_y)R)(D_0 + \hat{D}_1)C_x + (-2\,\kappa - 2){D_0}^2 \\ & + ((-2\,\kappa - 4)\hat{D}_1 + 2\,R(J + B_x))D_0 - 2\,\hat{D}_1^2 + 2\,\hat{D}_1\,(J + B_x)R \\ & - 2\,R^2(B_x\,C_y - B_y)\end{aligned} \tag{A.2b}$$

$$\begin{aligned}\beta_3 = {} & ((-\kappa^2 {C_y}^2 + (4\,JC_y + 4\,B_y - 4\,C_y)\kappa + 2\,J - 1){D_0}^2 \\ & + 4\,\hat{D}_1\,((JC_y + B_y - C_y)\kappa + J - 1/2)D_0 + 2\,(J - 1/2)\hat{D}_1^2){C_x}^2 \\ & + ((2\,\kappa^2 C_y + (-4\,J - 4\,B_x + 4\,C_y + 4)\kappa - 2\,J - 2\,B_x + 2){D_0}^2 \\ & + (((-4\,J - 4\,B_x + 4\,C_y + 4)D_1 - 4\,R(-B_x\,C_y + JC_y + 2\,B_y))\kappa \\ & + (-4\,J - 4\,B_x + 4)\hat{D}_1 - 2\,(J - B_x)R)D_0 - 2\,(R(-B_x\,C_y + JC_y + 2\,B_y)\kappa \\ & + \hat{D}_1\,(J + B_x - 1) + (J - B_x)R)\hat{D}_1)C_x + (-\kappa^2 - 4\,\kappa - 1){D_0}^2 \\ & + 4\,(\kappa + 1/2)(-\hat{D}_1 + R(J + B_x))D_0 + 2\,R(\hat{D}_1\,(J + B_x) \\ & - 2\,R(B_x\,C_y - B_y))\kappa - \hat{D}_1^2 + 2\,\hat{D}_1\,(J + B_x)R - 2\,R^2 B_x\end{aligned} \tag{A.2c}$$

$$\begin{aligned}\beta_4 = {} & -2\,((((-JC_y - B_y + C_y)\kappa - 2\,J + 1){C_x}^2 + ((J + B_x - C_y - 1)\kappa \\ & + 2\,J + 2\,B_x - 2)C_x + \kappa + 1){D_0}^2 + ((-2\,D_1\,J + \hat{D}_1){C_x}^2 \\ & + (R(-B_x\,C_y + JC_y + 2\,B_y)\kappa + (2\,J - 2\,B_x)R + 2\,\hat{D}_1\,(J + B_x - 1))C_x \\ & - R(J + B_x)\kappa + (-2\,J - 2\,B_x)R + \hat{D}_1)D_0 + (\hat{D}_1\,(J - B_x)C_x \\ & + R(B_x\,C_y - B_y)\kappa + 2\,RB_x - \hat{D}_1\,(J + B_x))R)\kappa\end{aligned} \tag{A.2d}$$

$$\begin{aligned}\beta_5 = {} & -2\,((1/2 + (-J + 1/2){C_x}^2 + (J + B_x - 1)C_x){D_0}^2 \\ & + ((J - B_x)C_x - J - B_x)RD_0 + R^2 B_x)\kappa^2\end{aligned} \tag{A.2e}$$

Matlab Code

B.1 Driver: Full T-cell Model and Reduced T-cell Model

Listing B.1: `DriverTcell.m`

```
%% Modeling MPN: Simulations of full vs. reduced model
% Initialize constants and variables
Initialize
Z     = [X0;X1;Y0;Y1;S;A];    % Full model
Zr    = [X0;Y0];              % Reduced model
tspan = [0 80*365/tbar];      % Dimensionless time

% Dimensionless Parameters from article
D0  = [0.5,1.00,1.52,1.8];
D1  = [0.1,0.5,1,5];
p = [rx,ry,ax,ay,Ax,Ay,dx0,dy0,dx1,dy1,cxx,cxy,cyx,cyy,es,ea,rs,I,rm];

figure
for i = 1:length(D1)
% Updating parameter choice
p2 = [R,J,D0(2),D1(i),Cx,Cy,Bx,By];
p3 = [p,p2];

% Full model
[t,sol]    = ode15s(@dl,tspan,Z,[],p3);
time       = t/365*tbar;

% Reduced model
[tr,solr]  = ode45(@dlr,tspan,Zr,[],p2);
timer      = tr/365*tbar;

% Plot of the solution
subplot(2,2,i)
plot_cancer(time,sol(:,1)*x0bar,sol(:,3)*y0bar,1)
hold on
plot_cancer(timer,solr(:,1)*x0bar,solr(:,2)*y0bar,3,'--')
title(sprintf('$D_1 = %0.1f$',D1(i)),'interprete','latex')
set(gca,'fontsize',20)
if i == 1
    h1 = plot(NaN,NaN,'b--','linewidth',3);
    h2 = plot(NaN,NaN,'r--','linewidth',3);
 HL = legend([h1,h2],'HSC','MSC');
 set(HL,'interprete','latex','location','northwest','fontsize',18)

end
set(gcf,'units','points','position',[300,300,800,500])
end
```

B.2 The Dimensionless Full T-cell Model

Listing B.2: `dl.m`

```
function dfdt = dl(t,IC,p)
% function: dfdt = dlr(t,IC,p)
%
% The full dimensionless T–cell model
% Katrine Ottesen Bangsgaard, May 2018
%
% Inputs:
% t     : Time
% IC    : Initial conditions: [X0 Y0]
% p     : Parameters p = [rx, ry, ax, ay, Ax, Ay, dx0, dy0, dx1, dy1,
%                         cxx, cxy, cyx, cyy, es, ea, rs, I, rm, R, J,
%                         D0, D1, Cx, Cy, Bx, By];
%
% Output:
% dfdt :  [X0dot; X1dot; Y0dot; Y1dot; Sdot; Adot]

% Unwrapping parameters
rx = p(1);
ry = p(2);
ax = p(3);
ay = p(4);
Ax = p(5);
Ay = p(6);
dx0= p(7);
dy0= p(8);
dx1= p(9);
dy1= p(10);
cxx= p(11);
cxy= p(12);
cyx= p(13);
cyy= p(14);
es = p(15);
ea = p(16);
rs = p(17);
I  = p(18);
rm = p(19);

% Dimensionless parameters
R = p(20);
J = p(21);
D0= p(22);
D1= p(23);
Cx= p(24);
Cy= p(25);
Bx= p(26);
By= p(27);

sbar = (dx0+ax)/rx;
eps1 = rx/dx1*sbar;
```

```
50 eps2 = rx/es*sbar;
51 eps3 = es/(ea*sbar);
52 eps4 = eps2*eps3;
53
54 % Initial conditions
55 X0 = IC(1);
56 X1 = IC(2);
57 Y0 = IC(3);
58 Y1 = IC(4);
59 S  = IC(5);
60 A  = IC(6);
61
62 % Model
63 X0dot = (S./(1 + X0+Cy*Y0) -1) * X0 ;
64 X1dot = (X0-X1)/eps1;
65 Y0dot = (R*S./(1 + Cx*X0+Y0) -D0 - D1*Y0) * Y0 ;
66 Y1dot = dy1/dx1*(Y0-Y1)/eps1;
67 Sdot  = (A-S+2*J)/eps2;
68 Adot  = (2*Bx*X0+2*By*Y0-A*S)/eps4;
69
70 % Output
71 dfdt  = [X0dot; X1dot; Y0dot; Y1dot; Sdot; Adot];
72
73 end
```

B.3 The Dimensionless Reduced T-cell Model

Listing B.3: `dlr.m`

```
1  function dfdt = dlr(t,IC,p)
2  % function: dfdt = dlr(t,z0,parameter)
3  %
4  % The dimensionless T-cell model
5  % Katrine Ottesen Bangsgaard, May 2018
6  %
7  % Inputs:
8  % t    : Time
9  % IC   : Initial conditions: [X0 Y0]
10 % p    : Parameters p = [R, J, D0, D1, Cx, Cy, Bx, By]
11 %
12 % Output:
13 % dfdt : [X0dot; Y0dot];
14
15 % Unwrapping parameters
16 R = p(1);
17 J = p(2);
18 D0= p(3);
19 D1= p(4);
20 Cx= p(5);
```

```
Cy= p(6);
Bx= p(7);
By= p(8);

% Initial conditions
X0 = IC(1);
Y0 = IC(2);

% Model
X0dot = (  (J+sqrt(J^2+2*Bx*X0+2*By*Y0))./(1+X0+Cy*Y0) -1) ...
        * X0;
Y0dot = (R*(J+sqrt(J^2+2*Bx*X0+2*By*Y0))./(1+Cx*X0+Y0) -D0 ...
        -D1*Y0) * Y0;

% Output
dfdt  = [X0dot; Y0dot];

end
```

B.4 Driver: Modified T-cell Model

Listing B.4: `DriverModifiedTcell.m`

```
pink        = [0.9 0.7 0.9];
blue        = [0   0.8 0.8];
green       = [0   1   0.1];
purple      = [0.7 0.6 1  ];
orange      = [1   0.7 0.4];
col         = [pink; blue; green; orange; purple];

% Load standard parameters initializing
Initialize

Zr    = [X0;Y0];              % IC
tspan = [0 80*365/tbar];      % Dimensionless time

% Dimensionless Parameters from article
D1    = [0.1 0.5 1 5];
kappa = [0.01 0.1 1 10];


%% Experiment 1: Fix the ratio between D1hat and kappa
figure
for j = 1:4
% T-cell Model
p          = [R,J,D0(2),D1(j),Cx,Cy,Bx,By];
[tr,solr]  = ode15s(@dlr,tspan,Zr,[],p);
timer      = tr/365*tbar;

```

```
subplot(2,2,j)
plot(timer,solr(:,1)*x0bar,'linewidth',3,'color','blue');

ylim([0 30000])
xlim([0 timer(end)])
hold on
plot(timer,solr(:,2)*y0bar,'linewidth',3,'color','red');
title(sprintf('$D_1 = %0.1f$',D1(j)),'interprete','latex')
set(gca,'fontsize',20)
grid on


for i = 1:length(kappa)
% Modified T-cell Model
p          = [R,J,D0(2),D1(j)*kappa(i),Cx,Cy,Bx,By,kappa(i)];
[tt,solt]  = ode15s(@dlr_tcell,tspan,Zr,[],p);
timet      = tt/365*tbar;

% Plot of solution
subplot(2,2,j)
plot(timet,solt(:,2)*y0bar,':','linewidth',3,'color',col(i+1,:));
hold on
plot(timet,solt(:,1)*x0bar,'--','linewidth',3,'color',col(i+1,:))

if j > 2
    xlabel('time [year]','interprete','latex')
end
if j == 1 && i == 4
h(1) = plot(NaN,NaN,'linewidth',3,'color',col(2,:));
h(2) = plot(NaN,NaN,'linewidth',3,'color',col(3,:));
h(3) = plot(NaN,NaN,'linewidth',3,'color',col(4,:));
h(4) = plot(NaN,NaN,'linewidth',3,'color',col(5,:));
l = legend([h(1) h(2) h(3) h(4)], ['$\kappa = $ ', ...
    num2str(kappa(1))], ['$\kappa = $ ', num2str(kappa(2))],...
    ['$\kappa = $ ', num2str(kappa(3))], ['$\kappa = $ ',...
     num2str(kappa(4))]);
 set(l,'location','southeast','interprete','latex','fontsize',18)
end
end
set(gcf,'units','points','position',[300,300,800,500])
end
%% Experiment 2: Change kappa
kappa = [0.01 0.1 1 10];
D1 = [0.1 0.5 1 5];
figure
for j = 1:length(D1)
    subplot(2,2,j)
for i = 1:length(kappa)
% The Modified T-cell Model
p          = [R,J,D0(2),D1(j),Cx,Cy,Bx,By,kappa(i)];
[tt,solt]  = ode45(@dlr_tcell,tspan,Zr,[],p);
timet      = tt/365*tbar;

plot(timet,solt(:,1)*x0bar,'--','linewidth',3,'color',col(i+1,:));
hold on
```

```
plot(timet,solt(:,2)*y0bar,':','linewidth',3,'color',col(i+1,:))

if j > 2
    xlabel('time [year]','interprete','latex')
end

if j == 1 && i == 1
h(1) = plot(NaN,NaN,'linewidth',3,'color',col(2,:));
h(2) = plot(NaN,NaN,'linewidth',3,'color',col(3,:));
h(3) = plot(NaN,NaN,'linewidth',3,'color',col(4,:));
h(4) = plot(NaN,NaN,'linewidth',3,'color',col(5,:));
l = legend([h(1) h(2) h(3) h(4)],['$\kappa = $ ', ...
    num2str(kappa(1))],['$\kappa = $ ', num2str(kappa(2))], ...
    ['$\kappa = $ ', num2str(kappa(3))],  ['$\kappa = $ ',...
     num2str(kappa(4))]);
  set(l,'interprete','latex','location','southeast')
end

ylim([0 30000])
xlim([0 timet(end)])
hold on
title(sprintf('$$\\hat{D}_1 = %g$$',D1(j)),'Interprete','Latex')
set(gca,'fontsize',20)
grid on
end
set(gcf,'units','points','position',[300,300,800,500])
end

%% study effect of kappa

x =linspace(0,10,1000);

k = [0.01, 0.1, 1, 10];
figure
%plot(x,x,'linewidth',2)

for i = 1:length(k)
h(i) = plot(x,1./(k(i)+x).*x,'--','linewidth',2,'color',col(i+1,:));
hold on
plot(x,1./k(i)*x,'color',col(i+1,:),'linewidth',2);
set(gca,'fontsize',18)

end
hold off
%ylabel('$\frac{1}{\kappa+Y_0}Y_0$','interprete','latex','fontsize',24)
xlabel('$y_0$','interprete','latex','fontsize',24)
hl = legend(h,'$\eta = 0.01$','$\eta = 0.1$',...
'$\eta = 1$','$\eta = 10$');
set(hl,'interprete','latex','location','northwest','fontsize',20)
xlim([0 2])
ylim([0 2])
%%
```

B.5 The Dimensionless Modified T-cell Model

Listing B.5: `dlrtcell.m`

```
function dfdt = dlrtcell(t,IC,parameter)
% function: dfdt = dlr_tcell(t,z0,parameter)
%
% The dimensionless modified T-cell model
% Katrine Ottesen Bangsgaard, May 2018
%
% Inputs:
% t     : time
% IC    : Initial conditions: [X0 Y0]
% p     : Parameters p = [R, J, D0, D1, Cx, Cy, Bx, By,K];
%
% Output:
% dfdt : [X0dot; Y0dot];

% Unwrapping parameters
R = parameter(1);
J = parameter(2);
D0= parameter(3);
D1= parameter(4);
Cx= parameter(5);
Cy= parameter(6);
Bx= parameter(7);
By= parameter(8);
K = parameter(9);

% Initial conditions
X0 = IC(1);
Y0 = IC(2);

% Model
X0dot = (  (J+sqrt(J^2+2*Bx*X0+2*By*Y0))./(1+X0+Cy*Y0) -1) * X0;
Y0dot = (R*(J+sqrt(J^2+2*Bx*X0+2*By*Y0))./(1+Cx*X0+Y0) ...
          -D0-D1*(1./(K+Y0))*Y0) .* Y0;
% Output
dfdt  = [X0dot; Y0dot];

end
```

B.6 Driver: Resistant T-cell Model

Listing B.6: `DriverResistantTcell.m`

```
% Driver for the Resistant T-cell Model
```

```
2
3  % Load standard parameters initializing
4  pink         = [0.9 0.7 0.9];
5  blue         = [0   0.8 0.8];
6  green        = [0   1   0.1];
7  purple       = [0.7 0.6 1  ];
8  orange       = [1   0.7 0.4];
9  col          = [pink; blue; green; orange; purple];
10
11 Initialize
12
13 Z0    = 0;                    % Resistant cells
14 Zr    = [X0;Y0;Z0];           % IC for resistant model
15 Z     = [X0;Y0];              % IC for T-cell  model
16 tspan = [0 80*365/tbar];      % Dimensionless time
17
18 % Dimensionless Parameters from article
19 D1  = [1,1.5,5,10];
20 P   = 1e-4;
21
22 figure
23 for i = 1:length(D1)
24 % Updating parameter choice
25 parameter = [R,J,D0,D1(i),Cx,Cy,Bx,By,P];
26
27 % Reduced model without resistance
28 [t,sol]   = ode45(@dlr,tspan,Z,[],parameter);
29 time      = t/365*tbar;
30 % Resistance 1
31 [tr,solr]  = ode45(@dlr_res,tspan,Zr,[],parameter);
32 timer      = tr/365*tbar;
33
34 % Plot of the solution
35  subplot(2,2,i)
36 h1 =plot(timer,x0bar*solr(:,1),'b--','linewidth',3);
37 hold on
38 h4 = plot(timer,y0bar*(solr(:,2)+solr(:,3)),'r--','linewidth',3);
39 h2 = plot(timer,y0bar*solr(:,2),'g-.','linewidth',3);
40 h3 = plot(timer,y0bar*solr(:,3),'-.','linewidth',3,'color',col(4,:));
41 plot(time,x0bar*sol(:,1),'b','linewidth',1)
42 plot(time,y0bar*sol(:,2),'r','linewidth',1)
43 title(sprintf('$D_1 = %0.1f$',D1(i)),'interprete','latex')
44 set(gca,'fontsize',20)
45 grid on
46 ylim([0 max(max(y0bar*(solr(:,2)+solr(:,3)),max(x0bar*(solr(:,1)))))])
47 if i > 2
48 xlabel('time [year]','interprete','latex')
49 end
50 set(gcf,'units','points','position',[300,300,800,500])
51 if i ==1
52  HL = legend([h1,h4,h3,h2],'HSC','MPN','R','NON R');
53  set(HL,'interprete','latex','location','northwest','fontsize',18)
54 end
55 end
```

B.7 The Dimensionless Resistant T-cell Model

Listing B.7: `dlrres.m`

```
function dfdt = dlr_res(t,IC,p)
% function: dfdt = dlr_res(t,z0,parameter)
%
% The dimensionless resistant T-cell model
% Katrine Ottesen Bangsgaard, May 2018
%
% Inputs:
% t     : time
% IC    : Initial conditions: [X0 Y0 Z0]
% p     : Parameters p = [R, J, D0, D1, Cx, Cy, Bx, By,P];
%
% Output:
% dfdt : [X0dot; Y0dot; Z0dot];

% Unwrapping parameters
R = p(1);
J = p(2);
D0= p(3);
D1= p(4);
Cx= p(5);
Cy= p(6);
Bx= p(7);
By= p(8);
P = p(9);

% Initial conditions
X0 = IC(1);
Y0 = IC(2);
Z0 = IC(3);

% Model
X0dot = (  (J+sqrt(J^2+2*Bx*X0+2*By*(Y0+Z0)))./(1+X0+Cy*(Y0+Z0)) -1)...
         * X0;
Y0dot = (R*(J+sqrt(J^2+2*Bx*X0+2*By*(Y0+Z0)))./(1+Cx*X0+(Y0+Z0))  ...
          -D0-D1*Y0) * Y0-P * Y0;
Z0dot = (R*(J+sqrt(J^2+2*Bx*X0+2*By*(Y0+Z0)))./(1+Cx*X0+(Y0+Z0))...
          -D0) * Z0 + P * Y0;

% Output
dfdt  = [X0dot; Y0dot;Z0dot];

end
```

B.8 Initialize

Listing B.8: `Initialize.m`

```
% Initialize the system with

% Parameters
rx = 8.7*1e-4;  % unit: day^-1
ry = 1.3*1e-3;  % unit: day^-1
ax = 1.1*1e-5;  % unit: day^-1
ay = 1.1*1e-5;  % unit: day^-1
Ax = 4.7*1e+13; % unit: -
Ay = 4.7*1e+13; % unit: -
dx0= 2*1e-3;    % unit: day^-1
dy0= 2*1e-3;    % unit: day^-1
dx1= 129;       % unit: day^-1
dy1= 129;       % unit: day^-1
cxx= 5.6*1e-5;  % unit: -
cxy= 5.4*1e-5;  % unit: -
cyx= 5.2*1e-5;  % unit: -
cyy= 5.0*1e-5;  % unit: -
es = 2;         % unit: day^-1
ea = 2*1e+9;    % unit: day^-1
rs = 3*1e-4;    % unit: day^-1
I  = 7;         % unit: day^-1
rm = 0;         % unit:

% Dimensionless constants
sbar = (dx0+ax)/rx;
abar = es/rs*sbar;
x0bar= 1/cxx;
x1bar= ax*Ax/(cxx*dx1);
y0bar= 1/cyy;
y1bar= ay*Ay/(cyy*dy1);
tbar = 1/(dx0+ax);

% Dimensionless Parameters from article
R   = 1.49;
J   = 0.76;
D0  = 1.00;
D1  = 0.10;
Cx  = 0.93;
Cy  = 1.08;
Bx  = 0.06;
By  = 0.07;

% Initial conditions from steady state
alphax  = (ax+dx0)/rx;
betax   = ax*Ax+dx0;
cetaH2  = betax*rs/(ea*es*cxx);
cetaH1  = I/es+cetaH2/alphax;

sHp     = (cetaH1+sqrt(cetaH1^2-4*cetaH2))/2;
aHp     = (es*sHp-I)/rs;
x0Hp    = (sHp-alphax)/(alphax*cxx);
x1Hp    = ax*Ax/dx1*x0Hp;
y0Hp    = 0;
```

```
y1Hp    = 0;

% Steady state
s       = sHp;
a       = aHp;
x0      = x0Hp;
x1      = x1Hp;
y0      = 1;
y1      = y1Hp;

% Dimensionless initial conditions
X0    = x0/x0bar;
X1    = x1/x1bar;
Y0    = y0/y0bar;
Y1    = y1/y1bar;
S     = s/sbar;
A     = a/abar;
```